CDF/PHYS/ELECTROWEAK/CDFR/6601
Version 10.0
December 15, 2004

Measurement of $W\gamma$ and $Z\gamma$ Production at CDF in Run 2

D. Benjamin, Alfred Goshaw, Michael Kirby
Duke University, Physics Department, Durham, North Carolina 27708

Helen Hayward, Beate Heinemann
University of Liverpool, Liverpool, UK L69 3BX

Naho Tanimoto
Okayama University, Okayama 700-8530, Japan

Abstract

An update on the $W/Z+\gamma$ analysis is presented using about 200 pb^{-1}. The cross-sections for $W\gamma$ and $Z\gamma$ production are measured for $\Delta R_{l\gamma} > 0.7$ and photon $E_T > 7$ GeV and the kinematic distributions are compared to the Standard Model prediction. The $W\gamma$ cross section in electron and muon channels is measured to be 18.1 ± 1.6(stat.) $\pm\, 2.4$(syst.) $\pm\, 1.2$(lumi.) pb compared to the SM expectation of 19.3 ± 1.4(th.) pb. The $Z\gamma$ cross section is found to be 4.6 ± 0.5(stat) $\pm\, 0.2$(sys) $\pm\, 0.3$(lumi) pb compared to the theoretical prediction of 4.5 ± 0.3(th.) pb.

1 Introduction

The associated production of a vector boson and a photon is an ideal test of the triple gauge couplings which are precisely predicted by the Standard Model. Any deviation from the Standard Model prediction could indicate new physics, e.g. compositeness of the vector bosons. Several measurements were performed by the LEP collaborations [1], the DØ [2] and the Run I CDF collaboration [3].

We present an analysis of $W/Z+\gamma$ events using about 200 pb^{-1} of CDF run 2 data. This is an update of the previous analysis based on 72 pb^{-1} [4] and 127.8 pb^{-1} [5]. Apart from increasing the data sample we have extended the phase space by using CMX muons for the $W\gamma \to \mu\nu\gamma$ and $Z\gamma \to \mu\mu\gamma$ channels and plug electrons for the $W\gamma \to e\nu\gamma$ analyses. We also, for the first time, investigate the presence of the "Radiation Amplitude Zero".

2 Dataset

Offline code version 4.10.4 and Stntuple tag dev_240 are used for this analysis.

2.1 Data Samples

The events are selected from the inclusive high p_T lepton triggers `ELECTRON_CENTRAL_18`, `CMUP_18`, `CMX_18` and the *Plug*-W trigger `MET_PEM` between March 23, 2002 and end of September 6, 2003 (runs 141544-168889). We require the runs to have the "good run" (DQM version 4.0) bit set [6]. For the Central-Plug (CP) $Z+\gamma$ and the plug W analysis we require the the good run bit for the SVX due to the Phoenix track requirement. The triggers, datasets and luminosities for the individual analysis channels are listed in table 1.

Sample	L3 Trigger	Dataset	$\int \mathcal{L}dt$ (pb^{-1})
$W\gamma \to e\nu\gamma$ central	`ELECTRON_CENTRAL_18`	bhel08/09	201.8
$W\gamma \to e\nu\gamma$ plug	`MET_PEM`	bpel08/09	167.8
$W\gamma \to \mu\nu\gamma$ CMUP	`CMUP_18`	bhmu08/09	191.6
$W\gamma \to \mu\nu\gamma$ CMX	`CMX_18`	bhmu08/09	175.3
$Z\gamma \to ee\gamma$ CC	`ELECTRON_CENTRAL_18`	bhel08/09	201.8
$Z\gamma \to ee\gamma$ CP	`ELECTRON_CENTRAL_18`	bhel08/09	167.8
$Z\gamma \to \mu\mu\gamma$ CMUP	`CMUP_18`	bhmu08/09	191.6
$Z\gamma \to \mu\mu\gamma$ CMX	`CMX_18`	bhmu08/09	175.3

Table 1: L3 Trigger Path, Dataset name and integrated luminosity for each analysis channel.

2.2 Monte Carlo Samples

The generator chosen to create the Monte Carlo samples for this analysis was Baur and Berger's `WGAMMA` program [7]. The performance and validation of this MC generator is described in [8]. `WGAMMA` was used to generate unweighted events with $|\eta_{lepton}| < 10$, $E_T^{\gamma} > 5.0$ GeV, $|\eta^{\gamma}| < 10$, and $\Delta R(l,\gamma) > 0.2$. These very wide cuts make sure that they are far from our analysis cuts, and do not need to be concerned with smearing bias. The `WGAMMA` generator was interfaced with `PYTHIA` for modeling the parton showering, hadronisation and underlying event. The samples generated are listed in Table 2.

Sample	Events	$\mathcal{L}$ (fb^{-1})	σ (pb)
$W\gamma \to e\nu\gamma$	211,936	4.74	44.7
$W\gamma \to \mu\nu\gamma$	211,531	4.73	44.7
$W\gamma \to \tau\nu\gamma$	195,903	5.02	39.0
$Z\gamma \to \mu\mu\gamma$	113,443	9.70	11.7
$Z\gamma \to ee\gamma$	208,500	17.8	11.7

Table 2: Table of MC samples used for the analysis. The number of events, cross section (including the k-factor) and resulting integrated luminosity for each MC sample are given.

To account for NLO corrections to the $W\gamma$ and $Z\gamma$ processes we determine a photon E_T dependent k-factor which was determined using Baur's NLO calculation programs

[9] (see Figure 1). Since this NLO program only considers the s-, t- and u- channel contributions and not the Bremstrahlung off the lepton lines we apply the incl. W cross section k-factor of 1.36 to this process. This procedure was recommended to us by Baur and confirmed by Stirling and Signer. Every MC event is weighted with this factor and thus it is considered in the MC based acceptance calculation. The resulting overall k-factorfor these MC samples we are using is 1.38 for $W\gamma$ and 1.365 for $Z\gamma$. The cross sections given in table 2 assume these values.

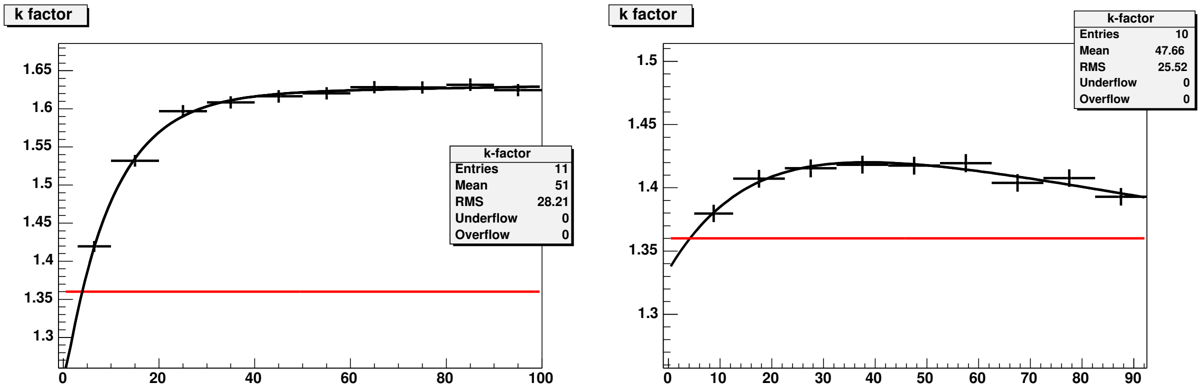

Figure 1: k-factor versus E_t^γ for $W\gamma$ (left) and $Z\gamma$ (right) production for the s-, t- and u-channel processes. The red line indicates the value for inclusive W production of 1.36.

3 Event Selection

We select one high p_T lepton and large missing transverse energy ($\not\!\!E_T$) to identify W bosons and two opposite charged leptons to identify Z bosons and follow closely the prescription of the inclusive W and Z cross section analysis [10, 11]. We use all lepton triggers available in CDF: central and plug electrons and CMUP and CMX muons. The lepton ID cuts are given in Tables 3 for *tight* leptons, 4 for *loose* leptons. For plug electrons we require a `PHOENIX` [12] track with at least 3 SVX or ISL hits attached. The selection of plug electrons are given in Table 5.

For plug electrons we additionally apply calibration factors which are determined from the central-plug Z mass peak. They are given in Table 6. The procedure is described in more detail in [13].

$\not\!\!E_T$ is calculated with respect to the highest p_T lepton z_0 value. It is also corrected for the muon momentum and for jets using *level 5* jet corrections. We require $\not\!\!E_T > 25$ GeV in the electron channel and $\not\!\!E_T$ >20 GeV in the muon channel for W candidates. Then calculate transverse mass, $M_T = \sqrt{2p_T^l \not\!\!E_T(1 - \cos\phi)}$, where $\cos\phi$ is the cosine between lepton and missing E_T , and require 30< M_T <120 GeV . For Z candidates, we require the invariant mass of the lepton pair to be greater than 40 GeV and less than 130 GeV. Further details on the inclusive W and Z selections are given in [13].

Table 3: Table of cuts to select tight electrons and muons. We constrain the tracks to the beamline(BC) and apply the curvature correction(LC) described in [10]. No explicit cut on the tight muon η is made but due to the requirement of a CMU or CMX stub, this corresponds to cut on detector $|\eta| < 1.0$.

<table>
<tr><th>Tight central Electron</th><th>CMUP Muon</th><th>CMX Muon</th></tr>
<tr><td>Good trigger electron</td><td colspan="2">Good trigger muon</td></tr>
<tr><td>$E_T > 25$ GeV</td><td colspan="2">$p_T > 20$ GeV</td></tr>
<tr><td>$|\eta| < 1.1$</td><td colspan="2"></td></tr>
<tr><td>$p_T > 10$ GeV</td><td colspan="2">Cosmic Ray removal</td></tr>
<tr><td>Track $|z_0| < 60$ cm</td><td colspan="2">Track $|z_0| < 60$ cm</td></tr>
<tr><td>N_{Ax} SL ≥ 3, N_{St} SL ≥ 3, with $\geq$7 hits</td><td colspan="2">N_{Ax} SL ≥ 3, N_{St} SL ≥ 3, with $\geq$7 hits</td></tr>
<tr><td>$E_{had}/E_{em} < 0.055 + 0.00045 \cdot E$</td><td colspan="2">$E_{em} < 2 + max(0, 0.0115 * (p - 100))$ GeV</td></tr>
<tr><td>$E/P < 2 || p_T > 50$ GeV</td><td colspan="2">$E_{had} < 6 + max(0, 0.028 * (p - 100))$ GeV</td></tr>
<tr><td>$Iso4/E_T < 0.1$</td><td colspan="2">$Iso4/p_T < 0.1$.</td></tr>
<tr><td>$\chi^2_{\text{strip}} < 10$</td><td colspan="2">$|d_0^{corr}| < 0.02(0.2)$ cm for SVX (COT) tracks</td></tr>
<tr><td>$-3.0 < q \cdot \Delta X < 1.5$ cm</td><td colspan="2">x-fiducial distance <0.0 cm</td></tr>
<tr><td>$|\Delta Z| < 3$ cm</td><td colspan="2">z-fiducial distance <-3.0 cm</td></tr>
<tr><td>$L_{shr} < 0.2$</td><td>$|\Delta X_{CMU}|$ <3cm</td><td>$|\Delta X_{CMX}|$ <6cm</td></tr>
<tr><td>$|X_{CES}|$ <21.0 cm</td><td>$|\Delta X_{CMP}|$ <5cm</td><td></td></tr>
<tr><td>9.0< $|Z_{CES}|$ <230.0 cm</td><td colspan="2">$\rho_{COT} > 140$ cm</td></tr>
<tr><td>Exclude Tower 9 and chimney</td><td>Bluebeam veto</td><td>Mini-skirt & Keystone veto</td></tr>
</table>

Table 4: "Loose" Lepton ID cuts for electrons (left) and muons (right).

Loose Central Electron	Loose Muon
$E_T > 25$ GeV	$p_T > 20$ GeV
$E_{had}/E_{em} < 0.055 + 0.00045 \cdot E$	$E_{em} < 2 + max(0, 0.0115 * (p - 100))$ GeV
$p_T > 10$ GeV	$E_{had} < 6 + max(0, 0.028 * (p - 100))$ GeV
$Iso4/E_T < 0.1$	$Iso4/p_T < 0.1$.
N_{Ax} SL ≥ 3, N_{St} SL ≥ 3, with $\geq$7 hits	N_{Ax} SL ≥ 3, N_{St} SL ≥ 3, with $\geq$7 hits
Track $\vert z_0\vert < 60$ cm	Track $\vert z_0\vert < 60$ cm
Track based fiducial requirement	$\vert d_0^{corr}\vert < 0.02(0.2)$ cm for SVX (COT) tracks
no Tower 9 or Chimney	$\Delta z_0 < 4.0$ cm

Table 5: Criteria used in the selection of the plug electron common to the W and Z samples.

Plug Electron	Tight Cuts	Loose Cuts
E_T	> 25 GeV	> 20 GeV
Had/Em	<0.05 for $E <= 100$ GeV, $< 0.05 + 0.026 \cdot \ln(E/100)$ for $E > 100$ GeV	
$Iso4/E_T$	< 0.1	
PES 5by9 u and v	> 0.65 for $E_T < 100$ GeV	
Fiducial base on PES	$1.2 < \|\eta\| < 2.8$	
PEM3x3 χ^2	< 10	
PEM Fit Towers	> 0	
Phoenix 2D Track	yes	if primary vertex, yes
NSvx Hits	>=3	>= 3

Table 6: Calibration factors for EAST and WEST Plug electrons for three different run ranges. These calibrations were measured using EM clusters that included the PPR energy, where the scaling was not applied to the PPR energy. An additional 2.6% for the east plug and 2.0% for the west plug was applied across all run ranges to compensate for this difference in cluster definition.

	run< 159600	159600 <run< 163600	run> 163600
EAST	1.036	1.071	1.089
WEST	1.031	1.066	1.096

As cross check we also performed measurements of the inclusive W and Z production cross sections and found good agreement between them and with NNLO calculations (see Table 3).

Table 7: $\sigma(W)\times B(W \to l\nu)$ and $\sigma(Z)\times B(Z \to l^+l^-)$ for the individual analysis channels. For the Z cross section the measurement was made for $66 < M_Z < 116$ GeV. The NNLO calculation for the W cross section is 2.73 nb and for the Z cross section for this mass range it is 252.9 pb.

$W \to l\nu$	σ (nb)
central e	2.70 ± 0.01 (stat) $\pm$ 0.07 (sys) $\pm$ 0.18 (lum)
plug e	2.57 ± 0.01 (stat) $\pm$ 0.13 (sys) $\pm$ 0.15 (lum)
CMUP μ	2.77 ± 0.01 (stat) $\pm$ 0.07 (sys) $\pm$ 0.18 (lum)
CMX μ	2.78 ± 0.02 (stat) $\pm$ 0.07 (sys) $\pm$ 0.18 (lum)
$Z \to l^+l^-$	σ (pb)
CC e	248 ± 4 (stat) $\pm$ 9 (sys) $\pm$ 15 (lum)
CP e	245 ± 4 (stat) $\pm$ 9 (sys) $\pm$ 15 (lum)
CMUP	256 $\pm$4 (stat)$\pm$9 (sys)$\pm$15 (lum)
CMX	256 $\pm$5 (stat)$\pm$9 (sys)$\pm$15 (lum)
CMUPX	253 $\pm$3 (stat)$\pm$9 (sys)$\pm$15 (lum)

3.1 Photon Selection

A photon is selected with $E_t > 7$ GeV and $\Delta R_{l\gamma} > 0.7$ and otherwise following the prescription of the photon group [14] given in table 3.1.

3.2 Acceptance and Efficiency of the Event Selection in MC

We simulated about 420,000 $W\gamma$ and 320,000 $Z\gamma$ events using the `WGAMMA` MC generator. They were simulated in the CDF detector using offline version 4.9.1 and reconstructed with the same offline code as the data (4.11.2+patches). The acceptance $\times$ efficiencies of the selection criteria described above are given in table 9. The final acceptance for the $W\gamma$ analysis is 1.50% for the muon and 1.13% for the electron channel. The acceptance of the cuts for the $Z\gamma$ analysis is given in table 10. The acceptance for the electron channel is 3.7% and 4.1% for the muon channel.

4 Background Processes

The following background processes are considered

- $W\gamma$ analysis
  - $Z\gamma \to ll\gamma$ is estimated using the MC used for the $Z\gamma$ analysis (see section 2.2)

Table 8: The list of photon selection cuts. (*) indicates a cut which was changed since the winter conference result.

cut variable	cut value
E_T	> 7.0 GeV
E_{had}/E_{em} (*)	$< 0.125 \vert\vert < 0.055 + 0.00045 \times E$
CES $(\chi^2_{wire} + \chi^2_{strip})/2$	< 20
CES $\vert x\vert$	< 21.0 cm
CES $\vert z\vert$	$9.0 < \vert z\vert < 230.0$ cm
2nd CES $<$ sliding	$< 0.14 \cdot E_T$ ($E_T < 18$)
	$< 2.4 + 0.01 \cdot E_T$ ($E_T > 18$)
Number of tracks pointing to em cluster	$N3D \leq 1$ and $p_t < 1 + 0.005 \cdot E_T$
Iso0.4 (*)	$Iso < 2.0 + 0.02 * (E_T - 20.0)$ ($E_T > 20$)
	$Iso/E_T < 0.1$ ($E_T < 20$)
TrackIso0.4 (*)	< 2 GeV (using tracks with $\vert z_0 - z_{lep}\vert < 5$ cm)

Table 9: Acceptance $\times$ efficiency after each requirement for the $W\gamma$ muon (CMUP and CMX) and electron (central and plug) channels.

Cut	$W\gamma \to \mu\nu\gamma$		$W\gamma \to e\nu\gamma$	
	(CMUP)	(CMX)	(central)	(plug)
none	100%	100%	100%	100%
lepton	7.22%	3.53%	10.05%	14.67%
$\not\!\!E_T > 20$ GeV	6.63%	3.26%	8.92%	7.67%
$30 < M_{trans} < 120$ GeV	6.58%	3.24%	8.83%	7.63%
γ ID cuts	1.70%	0.69%	1.94%	0.73%
$\Delta R > 0.7$	1.09%	0.49%	1.13%	0.69%

Table 10: Acceptance $\times$ efficiency after each requirement in $Z\gamma$ MC.

	$Z \to ee$		$Z \to \mu\mu$
Number of events	100%		100%
1 tight lepton	30.75%		27.35%
	central-central	central-plug	
1 loose lepton	5.66%	6.74%	8.75 %
Opposite Charge	5.54%	–	8.75 %
$40 < M_{ll} < 130$ GeV/c^2	5.42%	6.73%	8.07 %
photon cuts	1.03%	0.77%	1.94 %

- $W\gamma \rightarrow \tau\nu\gamma$ is estimated using the Standard Model MC (see section 2.2)
- W+jet with the jet faking a photon is estimated using the fake rate (see section 4.1). Note, that this estimate also includes the case where the W is faked by mis-measurements of jets
- fake $W + \gamma$ with the W being faked by mis-measurements of jets but a true photon (see section 4.2).

- $Z\gamma$ analysis
  - Z+jet with the jet faking a photon is estimated using the fake rate (see section 4.1). Note, that this estimate also includes the case where the W is faked by mis-measurements of jets
  - fake $Z + \gamma$ with the Z being faked by mis-measurements of jets but a true photon (see section 4.3).

4.1 Photon Fake Background

The method used to determine the background from jets fragmenting into a hard π^0 and then being misidentified as a photon is described in detail in [15]. An update of this determination including the new data and using the latest photon cuts and further systematic checks are described in [16]. The resulting "true" fake rate is shown in Figure 2.

We quote a systematic error of 30−80% on the fake depending on E_T^γ. This uncertainty arises from the differences between different method of determining the prompt photon contribution (see [16]) and from systematic checks performed on jet MC and data samples.

The fake rate is applied for any jet found in the inclusive W sample by weighting it correspondingly. The resulting background is about 30% in the $W\gamma \rightarrow e\nu\gamma$, 20% in the $W\gamma \rightarrow \mu\nu\gamma$ and 6% in the $Z\gamma$ analysis.

4.2 W Fake Background

An additional background may arise from the mis-measurement of jets faking a W boson. In the inclusive W analysis it was estimated to be 1.6±0.8% for the electron and 0.7±0.4% for the muon channel using the $\not{E}_T$ versus Iso4 method [10, 11]. In the previous $W\gamma$ analysis this was neglected. In order to verify that this background is indeed negligible compared to the photon fake background an new method is used.

For this method we assume that the background at $\not{E}_T < 10$ GeV scales the same way for the W and the $W\gamma$ analysis into the region of $\not{E}_T > 25(20)$ GeV for the electron (muon) channel. We have to subtract the part of the background from real "W"+ fake photon background since that is already taken into account. We remove Z candidates by requiring no 2nd electron (muon) candidate in the electron (muon) channel with $E_T > 25$ GeV ($p_T > 20$ GeV) since this background is taken into account using the $Z\gamma$ MC. Then

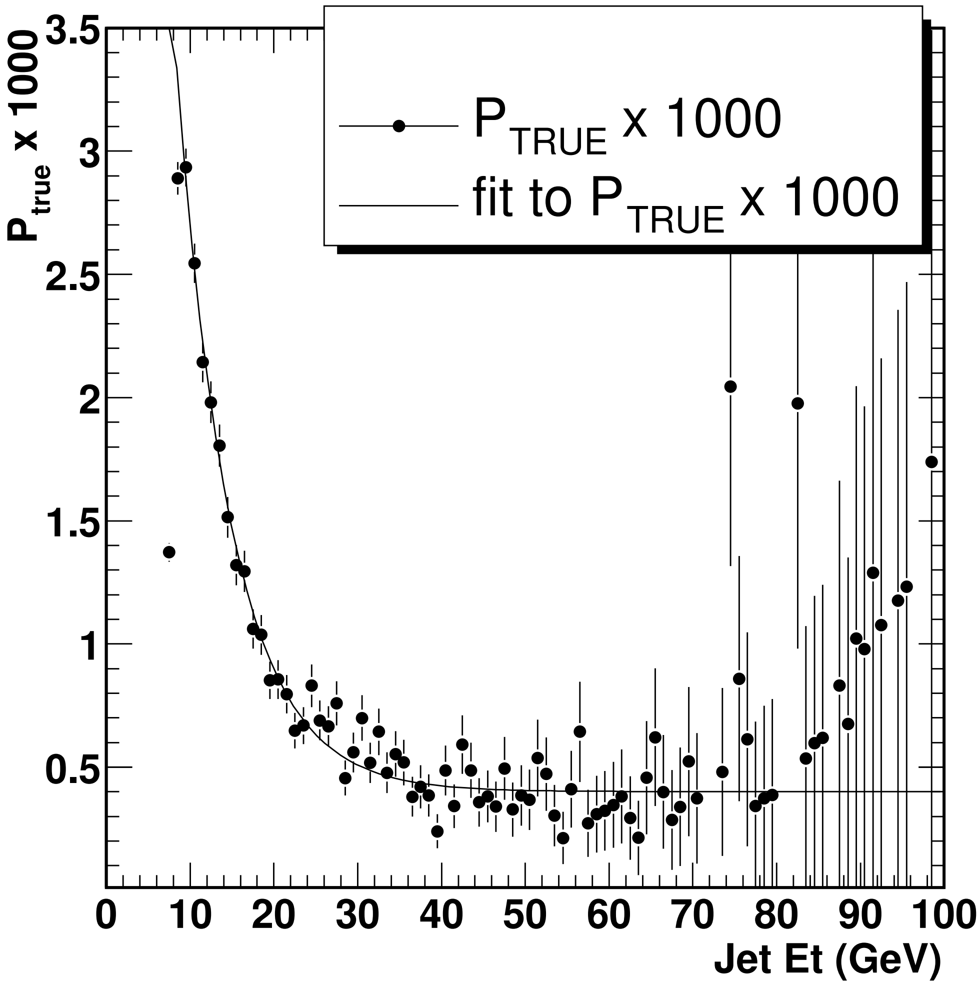

Figure 2: Probability of a jet faking a photon. Shown are the data (points) and the fit applied to $W/Z + jet$ samples to predict the amount of QCD background in our samples.

number of background events due to fake W's is given by $N_{W\gamma-BG} = \frac{N_A - N_B}{N_C} \cdot N_D$ where

$$\begin{aligned}
N_A &= \text{Events fulfilling } W\gamma \text{ event selection with } \not\!\!E_T < \not\!\!E_{T\ cut} \text{ GeV} \\
N_B &= \text{Events fulfilling } W\text{+fake } \gamma \text{ event selection with } \not\!\!E_T < \not\!\!E_{T\ cut} \text{ GeV} \\
N_C &= \text{Events fulfilling incl. } W \text{ event selection with } \not\!\!E_T < \not\!\!E_{T\ cut} \text{ GeV} \\
N_D &= \text{QCD Background events in incl. } W \text{ analysis}
\end{aligned}$$

The value of $\not\!\!E_{T\ cut}$ is varied in 5 GeV steps between 5 and 15 GeV and the resulting number of background events varies between -0.2 ± 2.3 and 1.5 ± 1.4 events. We have also repeated this study using ISO4/p_T instead of $\not\!\!E_T$ and find values between -0.4 ± 0.7 and 2.2 ± 1.1 for variations of the ISO4/p_T cut value between 0.2 and 0.4.

Additionally we analyzed 220 pb^{-1} of inclusive photon MC with $E_T > 15$ GeV and found no single event passing our full event selection. Therefore we can place an upper limit of < 2.7 events at 95% C.L. for a luminosity of 200 pb^{-1}. All indications are that this background is indeed negligible as assumed in the previous run 1 and 2 analysis [3,4]. We therefore neglect it.

4.3 Z Fake Background

In the $Z\gamma$ analysis there is also a contribution from background due to jets faking Z's. This is estimated using same-sign events. However, with the final selection cuts we have no single same sign event in either the electron or muon channel. In order to get a background estimate we loosen the electron identification cuts and assume that the additional background we are getting then scales between the inclusive Z sample and the $Z\gamma$ sample:

$$\frac{N_{ss}(Z\gamma)}{N_{ss}(Z)} = \frac{N_{ss}^{loose}(Z\gamma)}{N_{ss}^{loose}(Z)}$$

However, same-sign events can not only arise from QCD background but also from tridents. In order to estimate the background we subtract that contribution:

$$N_{Z-BG} = \frac{(N_{ss}(Z) - N_{ss,mc}(Z)) \times (N_{ss}^{loose}(Z\gamma) - N_{ss,mc}^{loose}(Z\gamma))}{(N_{ss}^{loose}(Z) - N_{ss,mc}^{loose}(Z))}$$

The resulting values are 0.2 ± 0.1 for CC and 0.0 ± 0.2 for CP $Z\gamma \to ee\gamma$ events. For the $Z\gamma \to \mu\mu\gamma$ we find no single event which has same-sign tracks even with loose cuts. We conclude that the background contribution due to a fake Z and a real photon is negligable compared to the fake photon contribution and the systematic errors due to the fake rate.

5 Efficiency Corrections

In this analysis, we use the Monte Carlo to determine the efficiency of the lepton and photon cuts. We correct the efficiency in the Monte Carlo to correspond to the data by applying the following corrections:

Trigger Efficiencies The electron trigger has an efficiency of 96.3% on average in the run range we consider (see [17]). The CMUP trigger efficiency is $88.7 \pm 0.7\%$ and the CMX trigger is $95.4 \pm 0.6\%$ efficient [18]. The `PEM20_MET15` trigger efficiency is parameterized as function of offline quantities $\not\!\!E_T$ and electron E_T. The details are given in [13]. The overall trigger efficiency for the $W\gamma \to e\nu\gamma$ event kinematics is 97.6%.

Lepton ID and Reconstruction Efficiencies Due to imperfect MC simulation there are correction factors to scale the MC to represent the efficiency measured in data:

- The ratio of the efficiency of central electron ID in Data versus MC was measured to be 0.964% [19]. The ratio of the efficiency of loose central electron ID in Data versus MC was measured to be 0.978%.
- The ratio of the muon reconstruction efficiencies between data and MC is $0.945 \pm 0.006\%$ for CMUP and $0.992 \pm 0.003\%$ for CMX muons [11, 18].
- The ratio of the muon ID efficiencies between data and MC is $0.939 \pm 0.007\%$ for CMUP and $1.015 \pm 0.008\%$ for CMX muons [11, 18].
- The ratio of the efficiencies of all plug electron ID cuts apart from the Phoenix track requirement between data and MC is 0.942 ± 0.011 [20]. The ratio of the efficiencies of the Phoenix track requirement between data and MC is 0.984 ± 0.006 [21]. Therefore the correction factor for plug electron ID is 0.927 ± 0.013.

Photon ID and Reconstruction Efficiency The efficiency of reconstructing photons in the simulation also differs from that in data. This is due to the larger amount of passive material in data and due to imperfect modeling of the photon ID variables:

- conversion rate: the photon ID cuts we use reject conversions due to the veto of tracks toward the EM tower. We estimated the efficiency loss for this analysis by determining the conversion rate in the simulation. It was found to be $10.21 \pm 0.25\%$. However, the material in the simulation is underestimated by about 30%. Presently the amount of material in the inner tracking volume at $R < 42$ cm is $15\% X_0$ and studies indicate that another $4.5 \pm 1.5\% X_0$ are present in the data [22]. Therefore the conversion probability in the data is estimated to be $13.3 \pm 1.0\% X_0$. Therefore we apply a correction factor to the simulation of $(100 - 13.3)/(100 - 10.2) = 0.97$ and assign a systematic error of 1.5%.
- the photon ID efficiency was measured using random cone studies, conversions and $Z \to ee$ events in [23] and [24]. Any disagreement between data and simulation in those studies was taken into account as a correction factor. A summary of those studies is given in table 5. The correction C_{iso} on the efficiency of $Iso4$ depends on E_T:

  For $E_T < 20$ GeV: $C_{iso} = 0.89 + 0.0175 \times E_T - 0.00104 \times E_T^2 + 2 \times 10^{-5} \times E_T^3$
  For $E_T \geq 20$ GeV: $C_{iso} = 0.98$
  On average this results in a correction factor of 0.972 for the $W\gamma$ MC photon E_T

Table 11: Correction factors determined from "random cone", conversion and $Z \to ee$ studies and their statistical errors. The calorimeter isolation cut correction depends on E_T. The last column gives the correction factor we use in the analysis and the associated systematic error.

Cut	Random Cone	Conversions	$Z \to ee$	Used value
Cal Iso	f(E_T)	–	1.010 ± 0.005	$f(E_T) \pm 0.01$
N3D	1.0 ± 0.003	–	0.977 ± 0.006	0.99 ± 0.01
Trk Iso	1.0 ± 0.003	–	0.988 ± 0.005	0.995 ± 0.005
χ^2_{CES}	–	1.01 ± 0.01	0.979 ± 0.004	0.99 ± 0.015
2nd CES	0.995 ± 0.01	1.01 ± 0.02	1.00 ± 0.003	1.00 ± 0.01
2nd CES	0.995 ± 0.01	0.99 ± 0.01	0.987 ± 0.004	0.99 ± 0.005

spectrum. The other photon efficiency correction factors result in a correction of 0.961 with a systematic error of 2%.

Efficiency of z_0 requirement The efficiency of the $|z_0| < 60$ cm cut is $95.0 \pm 0.004\%$ in data (see [25]). In MC we remove all events with $|z| > 60$ cm before performing the acceptance calculation.

For the plug W analysis the phoenix track requirement implies that a Z-vertex was found in the event (`ZVertexColl` [26, 27]). We estimate the efficiency of the z-vertex finder in data by using CP Z candidates and removing the track of the central electron from the algorithm. The resulting efficiency is $\epsilon_{12}^{data} = 91.3 \pm 0.3\%$ for class 12 and $\epsilon_0^{data} = 93.1 \pm 0.3$ for any ("class 0") vertex. In MC we measure $\epsilon_{12}^{MC} = 90.4 \pm 0.2\%$ for a class 12 and $\epsilon_0^{MC} = 96.5 \pm 0.1\%$ for any vertex. The Phoenix electron finder uses the highest $\sum p_T$ vertex of any class. We thus determine a scale factor of $\epsilon_0^{data}/\epsilon_0^{MC} = 0.965$ by which we correct the MC.

Tables 12 and 13 list the final values used to scale the MC expectation for the $W\gamma$ and $Z\gamma$ analysis respectively.

Table 12: Efficiency corrections applied to the `WGAMMA` MC. (*) This correction factor is depends on E_T: given here is the value excluding the E_T-dependent factor.

source	$W\gamma \to e\nu\gamma$		$W\gamma \to \mu\nu\gamma$	
	Central	Plug	CMUP	CMX
trigger	0.963	0.976	0.887	0.954
lepton ID and rec.	0.983	0.927	0.887	1.007
photon ID(*)	0.961	0.961	0.961	0.961
conversion rate	0.970	0.970	0.970	0.970

Efficiency of Cosmic tagger rejection We have quote the efficiency of cosmic tagger rejection to be 0.9999±0.0001 for $W\gamma$ and 0.9994±0.0006 for $Z\gamma$ [11].

Table 13: Efficiency corrections applied to the ZGAMMA MC. (*) This correction factor is depends on E_T: given here is the value excluding the E_T-dependent factor.

source	$Z\gamma \to ee\gamma$		$Z\gamma \to \mu\mu\gamma$	
	CC	CP	CMUP+MIP	CMX+MIP
trigger	0.999	0.963	0.892	0.956
lepton ID and rec.	0.966	0.911	0.887	1.007
photon ID(*)	0.961	0.961	0.961	0.961
conversion rate	0.970	0.970	0.970	0.970

6 Systematic errors

In this section, we discuss the systematic errors and their impact on the measurement. The following sources of systematic errors are considered:

- A 30-80% uncertainty on the photon fake rate is assigned (see [15]) depending on E_T. This leads to an uncertainty of 10% for the $W\gamma$ and 2% for the $Z\gamma$ analysis in the electron and to 8% for the $W\gamma$ and 2% for the $Z\gamma$ analysis in the muon channel.

- We attribute a 1% error for the muon ID and reconstruction efficiency [18] , a 1% error for the electron ID efficiency and a 2.5% error for the plug phoenix electron ID efficiency. This results in a 1% (2% plug) error in the $W\gamma$ and 2% in the $Z\gamma$ cross section.

- A 0.01% for $W\gamma$ and 0.06% for $Z\gamma$ uncertainty due to the cosmic rejection [11].

- 0.004% uncertainty due to the efficiency of the $|z_0| < 60$ cm cut [25].

- The photon ID efficiency was determined in three different ways: $Z \to ee$ events were used to check the efficiency at high E_T and the conversion electrons were used at low E_T [24]. The isolation cuts were additionally studied using random cones in the central calorimeter in W events transverse to the lepton plane [23]. A systematic error of 2% was determined from the comparison between the different samples (see Table 5).

- The uncertainty on the conversion rate is 1.5% (see section 5).

- The uncertainty on the trigger efficiencies for the central electron, plug electron, and muon triggers is 1%.

- Electron and muon energy scale uncertainties: the uncertainty on the energy and momentum scales is 1% [10,11]. This results in a 1(2)% error on the $W\gamma(Z\gamma)$ cross section. In the plug, the energy scaling uncertainty is 2%, which results in a 2.5% error on the $W\gamma$ cross section.

- The photon energy scale uncertainty is taken to be 3%. The electron energy scale has been verified to be 1% in the region of the Z mass. In order to account for possible non-linearities we increase the error to 3%. We are planning to reduce this in the future by utilizing J/ψ and Υ data. The resulting error on the $W\gamma$ and $Z\gamma$ cross sections is 3%.

- The acceptance uncertainty is determined to be 2% (2.5%) for $W\gamma$ ($Z\gamma$): It is evaluated in the MC by looking at the effect of unweighting events and the k-factor used to correct for NLO terms. The unweighting of events was done online during event generation and so has some inefficiency. This inefficiency was determined by generating 5 large samples and measuring the acceptance before and after unweighting. The effect of unweighting was less than 1%. Using Uli Baur's NLO `WGAMMA` program and the LO program, the acceptance for our analysis cuts was measured at the parton level. Determining the difference between the two acceptances gives the uncertainty. So, combining the two errors on acceptances give a total error of 3%. We also studied the effect of varying the PDF's of MRST on the cross section and found it to be negligible.

- The uncertainty in the luminosity is 6%.

The total experimental systematic error is about 10% for the $W\gamma$ analysis in the and 8% for the $Z\gamma$ analysis when excluding the luminosity error of 6%. The largest contributions comes from the photon fake rate which is fully correlated between the analysis channels.

The systematic errors and their propagation between electron and muon channels for $W\gamma$ and $Z\gamma$ analyses are summarised in Tables 14 and 15.

7 Standard Model Expectation

The Standard Model prediction and its uncertainty is described in detail in [8].

Three sources of systematic errors were considered: factorization scale, PDF uncertainty, and k-factor corrections.

- During the generation of events in the MC program, a lower limit is set on the factorization scale of the the process. This allows you to define two physics regimes, the high scale regime calculated by the `WGAMMA` generator, and a low scale regime which will be the initial state radiation done by a showering program. Usually, the factorization scale is set to the Q of the event. To study the effect that this scale has on the cross section, the Q scale was varied by a factor of 2. Comparing the calculated cross sections with these scales gave an error of 2%.

- The error on the cross sections from the uncertainty from the parton distribution functions was determined by using 6 different PDFs. The PDF used for the generation of events was CTEQ5L, while additional cross section predictions was made using 5 MRST PDF sets (72, 73, 74, 75, and 76 in the CERN `pdflib`). The error from this change of PDF was 5%.

- A k-factor is applied to the cross section to account for NLO corrections to the LO MC program. To estimate the error on the k-factor due to higher order contributions

Table 14: Systematic error summary for $W\gamma$. 'x' means that channel needs to take into account its systematic uncertainty.

source	(%)	Central	plug	CMUP	CMX
Jet fake	˜30.	x	x	x	x
Z_0 cut eff	1.	x	x	x	x
photon cut eff	2.	x	x	x	x
energy scale(γ)	3.	x	x	x	x
conversion rate uncertainty	1.5	x	x	x	x
momentum scale(μ)	2.			x	x
acceptance	1.	x	x		
acceptance	2.			x	x
central e ID	1.	x			
central e trigger	1.	x			
Energy scale (e)	1.	x	x		
plug e ID	2.5		x		
plug trig e	1.		x		
plug e vertex eff	1.		x		
plug e track eff	1.5		x		
cosmic	0.01			x	x
COT track reconstruction	0.4	x		x	x
CMUP ID	0.7			x	
CMUP reconstruction	0.6			x	
CMUP trigger	0.7			x	
CMX ID	0.8				x
CMX reconstruction	0.3				x
CMX trigger	0.6				x
luminosity	6.	x	x	x	x

Table 15: Systematic error summary for $Z\gamma$. 'x' means that channel needs to take into account its systematic uncertainty. '2x' means it is applied twice because Z has two legs.

Source	%	% effect on σ	CC	CP	CMUP	CMX
Jet Fake	30*Nbg	2	x	x	x	x
Z_0 cut eff	1	1	x	x	x	x
Photon cut eff	2	2	x	x	x	x
energy scale(γ)	3	2	x	x	x	x
conversion rate uncertainty	1.5	1.5	x	x	x	x
Momentum scale (μ)	2	1			x	x
acceptance	1.		x	x		
acceptance	2.5				x	x
Central e ID	1	1	x	x		
central e trigger	1	1	x	x		
central e Energy Scale	1	1	x2	x		
plug e ID	2.5	2.5		x		
plug e track eff	1.5	1.5		x		
cosmic	0.06	0.6			x	x
COT track reconstruction	0.4	0.4			x2	x2
CMUP ID	0.7	0.7			x	
CMUP reconstruction	0.6	0.6			x	
CMUP trigger	0.8	0.8			x	
CMX ID	0.8	0.8				x
CMX reconstruction	0.3	0.3				x
CMX trigger	0.6	0.6				x
Luminosity	6.0		x	x	x	x

the Q scale in the NLO calculation was varied by factors of 2. This results in a 3% variation of the SM prediction.

Adding all of these errors in quadrature results in a total error on the Standard Model prediction of 7%.

8 Results

In this section we present the results of the $W\gamma$ and $Z\gamma$ analysis, then show the kinematical distributions comparing with the Standard Model expectations.

8.1 $W\gamma$ Results

In the central electron channel 131 events are observed compared to a Standard Model expectation of $127.6 \pm 1.51(\text{stat.}) \pm 11.81(\text{sys.}) \pm 5.49(\text{lumi.})$. The 1st error is due to the experimental systematic uncertainties, the 2nd due to the 6% luminosity error and the 3rd due to the theoretical uncertainty on the cross section of 7%. In the plug electron channel 64 events are observed compared to a Standard Model expectation of $66.02 \pm 0.94(\text{stat.}) \pm 7.32(\text{sys.}) \pm 2.56(\text{lumi.})$. In the muon channel 128 events are observed compared to a Standard Model expectation of $142.4 \pm 1.51(\text{stat.}) \pm 9.35(\text{sys.}) \pm 6.89(\text{lumi.})$. Note that the error on the luminosity uncertainty and Standard Model expectations only affect the Monte Carlo predictions and not the QCD background estimate.

The observed and expected numbers of events for the electron and muon channels are listed in Tables 16 and 17 respectively.

Table 16: Expected and observed numbers of events in the $W\gamma \rightarrow e\nu\gamma$ analysis for central and plug electrons. Given are the statistical and the experimental systematic error.

	Number of Events	
	Central	Plug
$W\gamma \rightarrow e\nu\gamma$	$85.51 \pm 1.49(\text{stat.}) \pm 4.14(\text{sys.})$	$41.1 \pm 0.93(\text{stat.}) \pm 2.18(\text{sys.})$
W+jet	$36.14 \pm 0.10(\text{stat.}) \pm 11.06(\text{sys.})$	$23.39 \pm 0.10(\text{stat.}) \pm 7.00(\text{sys.})$
$W\gamma \rightarrow \tau\nu\gamma$	$0.93 \pm 0.15(\text{stat.}) \pm 0.05(\text{sys.})$	$0.60 \pm 0.11(\text{stat.}) \pm 0.03(\text{sys.})$
$Z\gamma \rightarrow ee\gamma$	$5.03 \pm 0.19(\text{stat.}) \pm 0.24(\text{sys.})$	$1.33 \pm 0.09(\text{stat.}) \pm 0.07(\text{sys.})$
total SM+BG	$127.6 \pm 1.51(\text{stat.}) \pm 11.81(\text{sys.})$	$66.02 \pm 0.94(\text{stat.}) \pm 7.32(\text{sys.})$
Data	131	64

The combined central and plug electron results, and combined CMUP and CMX muon results are given in Table 18. The combined electron and muon results are given in Table 19.

Figure 3, 4 and 5 show various kinematic distributions for the $W\gamma \rightarrow e\nu\gamma$ and $W\gamma \rightarrow \mu\nu\gamma$ candidates and the corresponding Standard Model expectations for the electron and muon channel respectively. The data are well described by the Standard Model expectation in all distributions. Figure 6 shows electron and muon combined distributions.

Table 17: Expected and observed numbers of events in the $W\gamma \to \mu\nu\gamma$ analysis for CMUP and for CMX muons. Given are the statistical and the experimental systematic error.

	Number of Events	
	CMUP	CMX
$W\gamma \to \mu\nu\gamma$	63.58 ± 1.17(stat.) ± 3.17(sys.)	31.60 ± 0.88(stat.) ± 1.57(sys.)
QCD background	17.89 ± 0.00(stat.) ± 4.90(sys.)	9.69 ± 0.00(stat.) ± 2.63(sys.)
$W\gamma \to \tau\nu\gamma$	1.44 ± 0.17(stat.) ± 0.07(sys.)	0.86 ± 0.14(stat.) ± 0.04(sys.)
$Z\gamma \to \mu\mu\gamma$	11.74 ± 0.26(stat.) ± 0.59(sys.)	5.63 ± 0.19(stat.) ± 0.28(sys.)
total SM+BG	94.66 ± 1.21(stat.) ± 6.17(sys.)	47.78 ± 0.91(stat.) ± 2.75(sys.)
Data	93	35

Table 18: Expected and observed numbers of events in combining the central and plug electron, and CMUP and CMX muon in $W\gamma \to l\nu\gamma$ analysis. Given are the statistical and the experimental systematic error.

	Number of Events	
	Electron	Muon
$W\gamma \to l\nu\gamma$	126.8 ± 1.49(stat.) ± 5.60(sys.)	95.18 ± 1.46(stat.) ± 4.69(sys.)
QCD background	59.53 ± 0.0(stat.) ± 18.05(sys.)	27.59 ± 0.0(stat.) ± 7.53(sys.)
$W\gamma \to \tau\nu\gamma$	1.50 ± 0.16(stat.) ± 0.07(sys.)	2.30 ± 0.22(stat.) ± 0.11(sys.)
$Z\gamma \to ll\gamma$	6.30 ± 0.18(stat.) ± 0.28(sys.)	17.37 ± 0.32(stat.) ± 0.90(sys.)
total SM+BG	194.1 ± 1.51(stat.) ± 19.0(sys.)	142.4 ± 1.51(stat.) ± 9.35(sys.)
Data	195	128

Table 19: Expected and observed numbers of events combining the electron and muon $W\gamma \to l\nu\gamma$ analysis. Given are the statistical and the experimental systematic error.

	Number of Events
$W\gamma \to l\nu\gamma$	221.9 ± 2.09(stat.) ± 9.45(sys.)
QCD background	87.12 ± 0.0(stat.) ± 25.58(sys.)
$W\gamma \to \tau\nu\gamma$	3.80 ± 0.27(stat.) ± 0.17(sys.)
$Z\gamma \to ll\gamma$	23.67 ± 0.37(stat.) ± 1.10(sys.)
total SM+BG	336.5 ± 2.14(stat.) ± 27.66(sys.)
Data	323

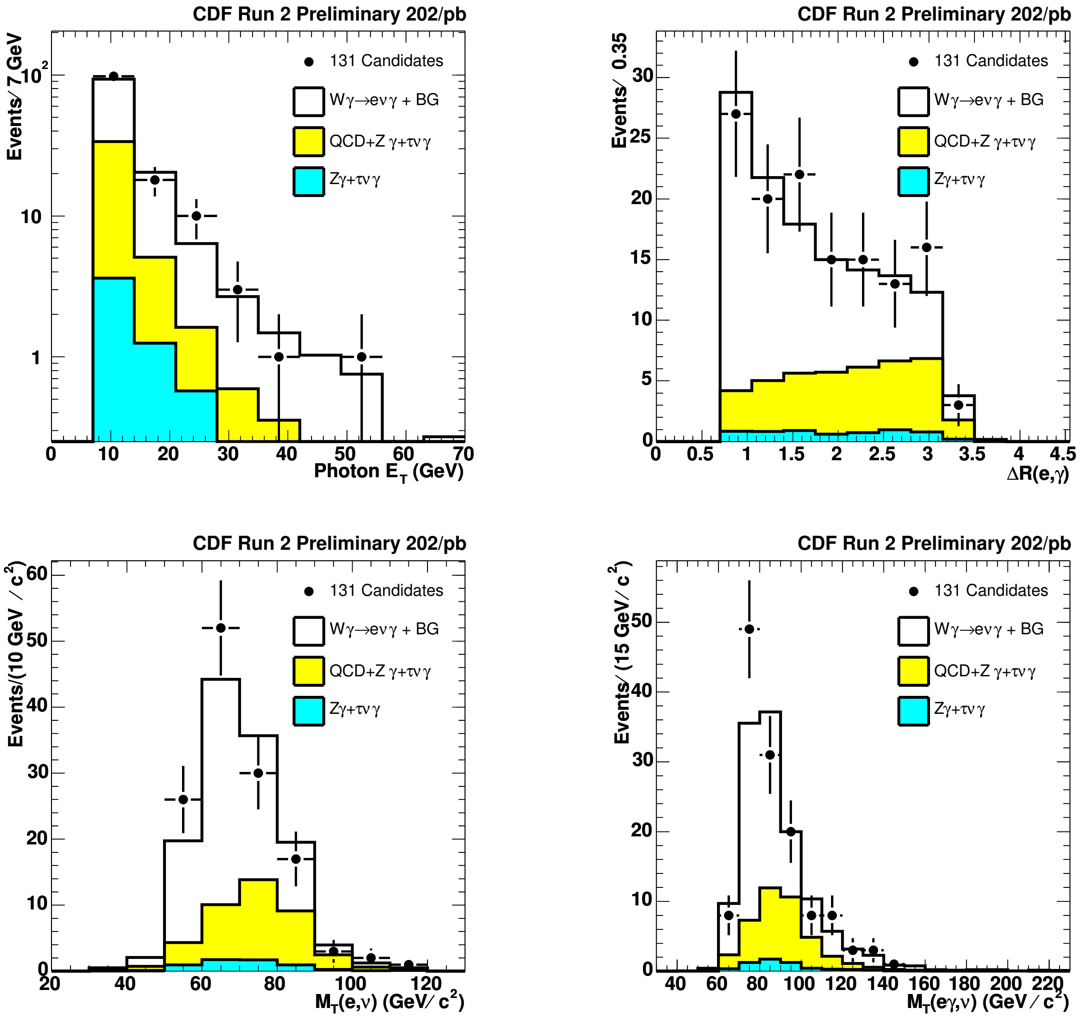

Figure 3: Several kinematic distributions for the data (points) and the Standard Model prediction (histogram) plus background expectation for the $W\gamma \to e\nu\gamma$ central electron channel. The dark blue histogram is the contribution for $W\gamma \to \tau\nu\gamma \to \bar{\nu}\nu\nu e\gamma$, the turquoise the sum of that and $Z\gamma \to ee\gamma$, the yellow the sum of all background contributions (QCD, $Z\gamma$ and $W\gamma \to \tau\nu\gamma$) and the open histogram the sum of the background and the $W\gamma \to e\nu\gamma$ signal expectation.

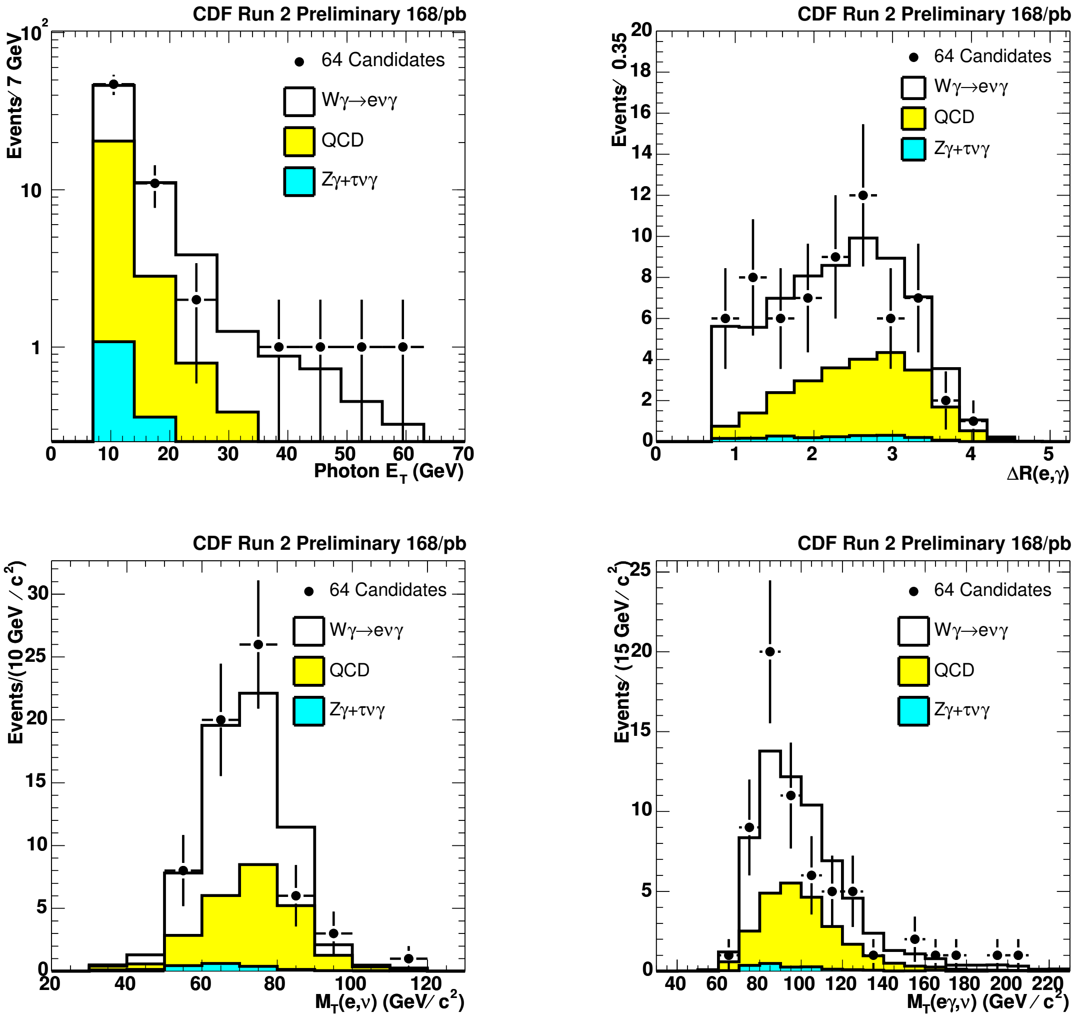

Figure 4: Several kinematic distributions for the data (points) and the Standard Model prediction (histogram) plus background expectation for the $W\gamma \to e\nu\gamma$ plug channel. The dark blue histogram is the contribution for $W\gamma \to \tau\nu\gamma \to \bar{\nu}\nu\nu e\gamma$, the turquoise the sum of that and $Z\gamma \to ee\gamma$, the yellow the sum of all background contributions (QCD, $Z\gamma$ and $W\gamma \to \tau\nu\gamma$) and the open histogram the sum of the background and the $W\gamma \to e\nu\gamma$ signal expectation.

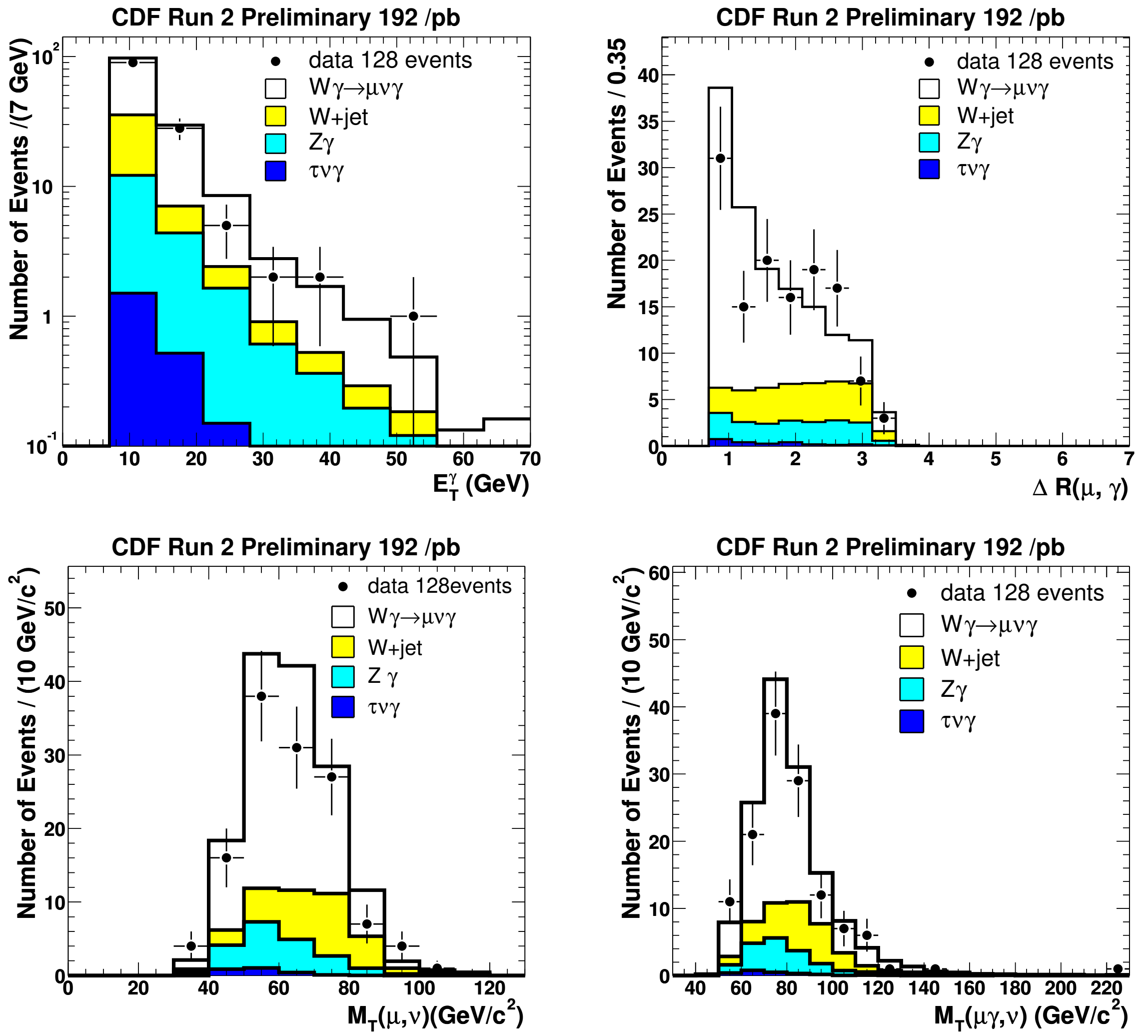

Figure 5: Several kinematic distributions for the data (points) and the Standard Model prediction (histogram) plus background expectation for the $W\gamma \to \mu\nu\gamma$ channel. The dark blue histogram is the contribution for $W\gamma \to \tau\nu\gamma \to \bar{\nu}\nu\nu\mu\gamma$, the turquoise the sum of that and $Z\gamma \to \mu\mu\gamma$, the yellow the sum of all background contributions (QCD, $Z\gamma$ and $W\gamma \to \tau\nu\gamma$) and the open histogram the sum of the background and the $W\gamma \to \mu\nu\gamma$ signal expectation.

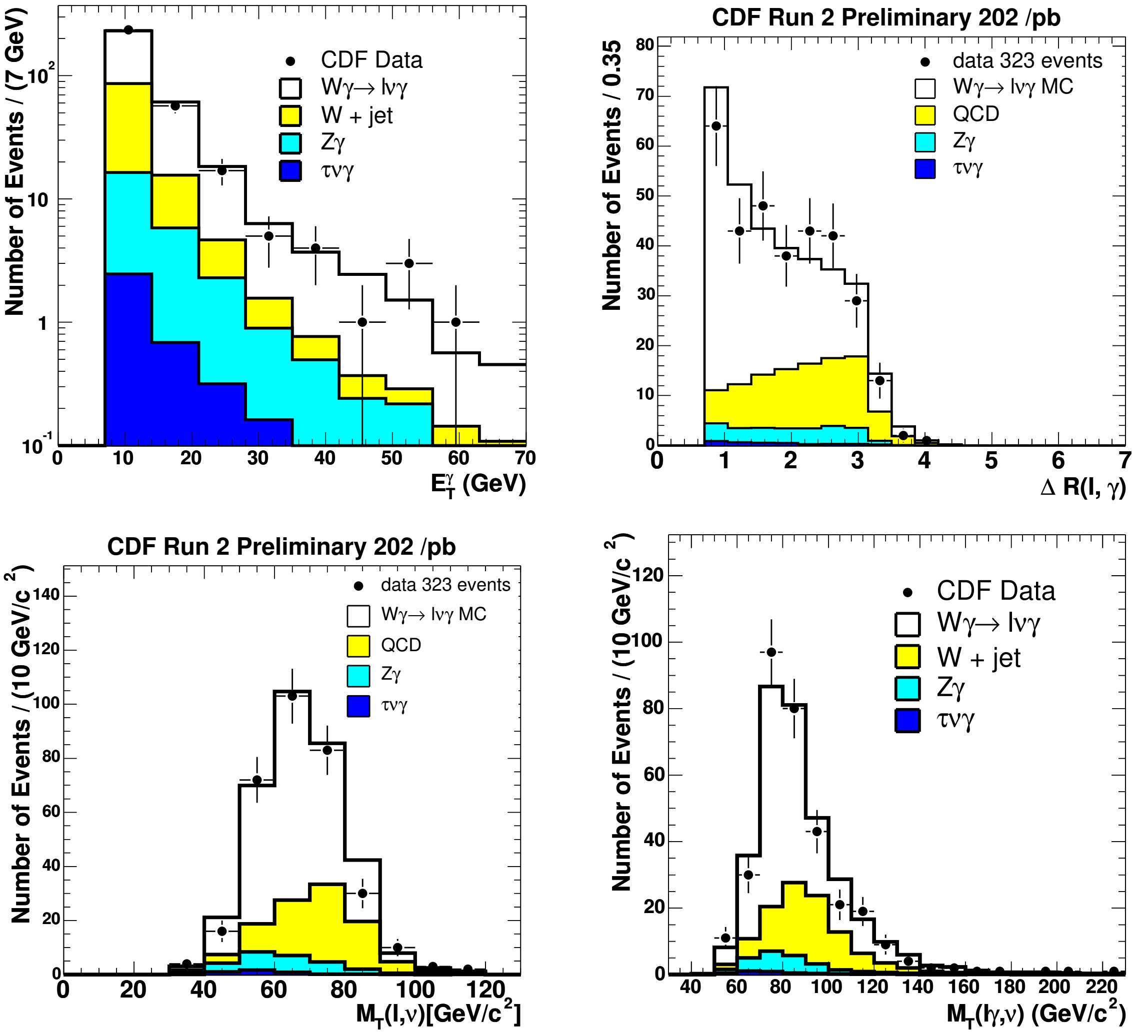

Figure 6: Several kinematic distributions for the data (points) and the Standard Model prediction (histogram) plus background expectation for the $W\gamma \rightarrow l\nu\gamma$ channels in the CEM, PEM, CMUP, and CMX. The dark blue histogram is the contribution for $W\gamma \rightarrow \tau\nu\gamma \rightarrow \bar{\nu}\nu\nu l\gamma$, the turquoise the sum of that and $Z\gamma \rightarrow ll\gamma$, the yellow the sum of all background contributions (QCD, $Z\gamma$ and $W\gamma \rightarrow \tau\nu\gamma$) and the open histogram the sum of the background and the $W\gamma \rightarrow l\nu\gamma$ signal expectation.

In Figure 7 the transverse mass is shown versus the cluster transverse mass. The events which correspond to final state radiation off the lepton line are likely to have $M_{CT} < 90$ GeV whilst the events from s-channel and initial state radiation diagrams are likely to have values above 90 GeV.

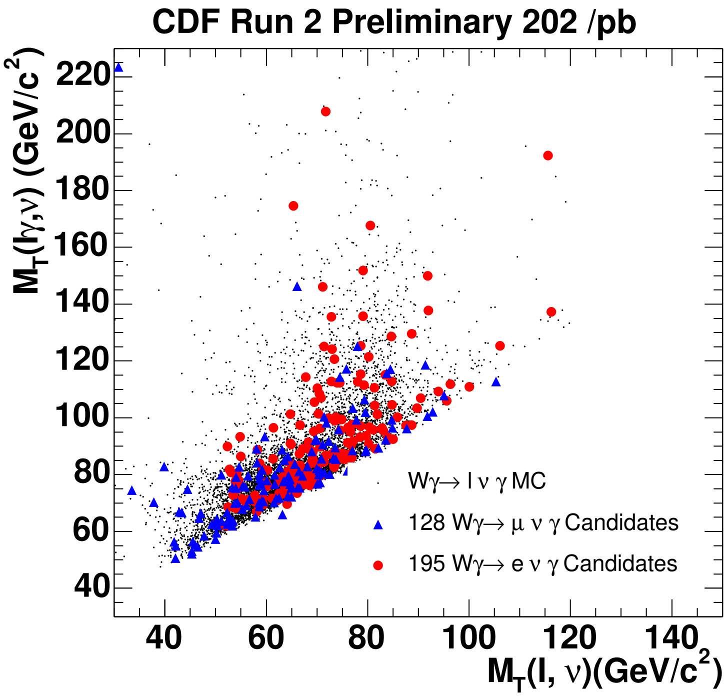

Figure 7: Cluster transverse mass versus transverse mass for the electron(red circle) and muon(blue triangle) channel.

8.2 $Z\gamma$ Results

The observed and expected numbers of events for the electron (CC and CP separately) and muon channels are listed in table 20. The combined result of all channels is shown in table 21. In total 71 events are observed compared to a Standard Model expectation of $69.8 \pm 3.0(\mathrm{sys}) \pm 3.9(\mathrm{lum.}) \pm 4.5(\mathrm{th.})$. The 1st error is due to the experimental systematic uncertainties, the 2nd due to the 6% luminosity error and the 3rd due to the theoretical uncertainty on the cross section of 7%.

For the combined result the systematic errors are combined fully taking into account correlations. The details of this combination can be found in appendix A.

Figures 8 and 9 show kinematic distributions of the $Z\gamma$ candidates in the electron and muon channel compared to the Standard Model expectation. All distributions are in good agreement with the expectation. The sum of the electron and muon channel is shown in Figure 10 and 11.

Figure 12 shows the E_t and $M(ll\gamma)$ distributions up to the highest values. There is one event at $E_t^\gamma = 140$ GeV and a mass of 380 GeV. It is difficult to quantify the background

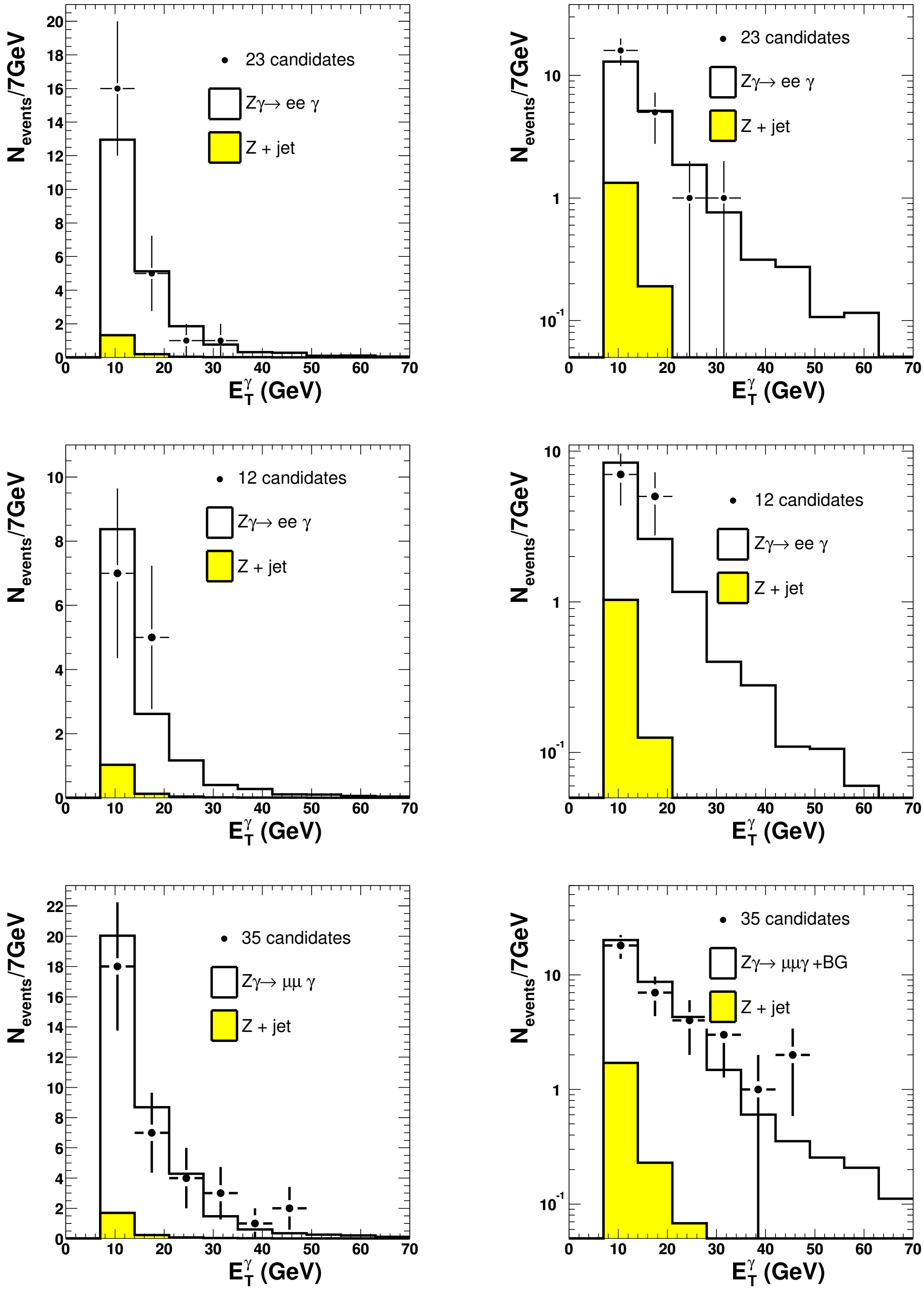

Figure 8: Photon E_T on linear (left) and logarithmic (right) scale for CC $Z \rightarrow ee$ (top), CP $Z \rightarrow ee$ (middle) and $Z \rightarrow \mu\mu$ candidates. The points are the data, the open histogram the Standard Model expectation and the shaded histogram is the estimated QCD background.

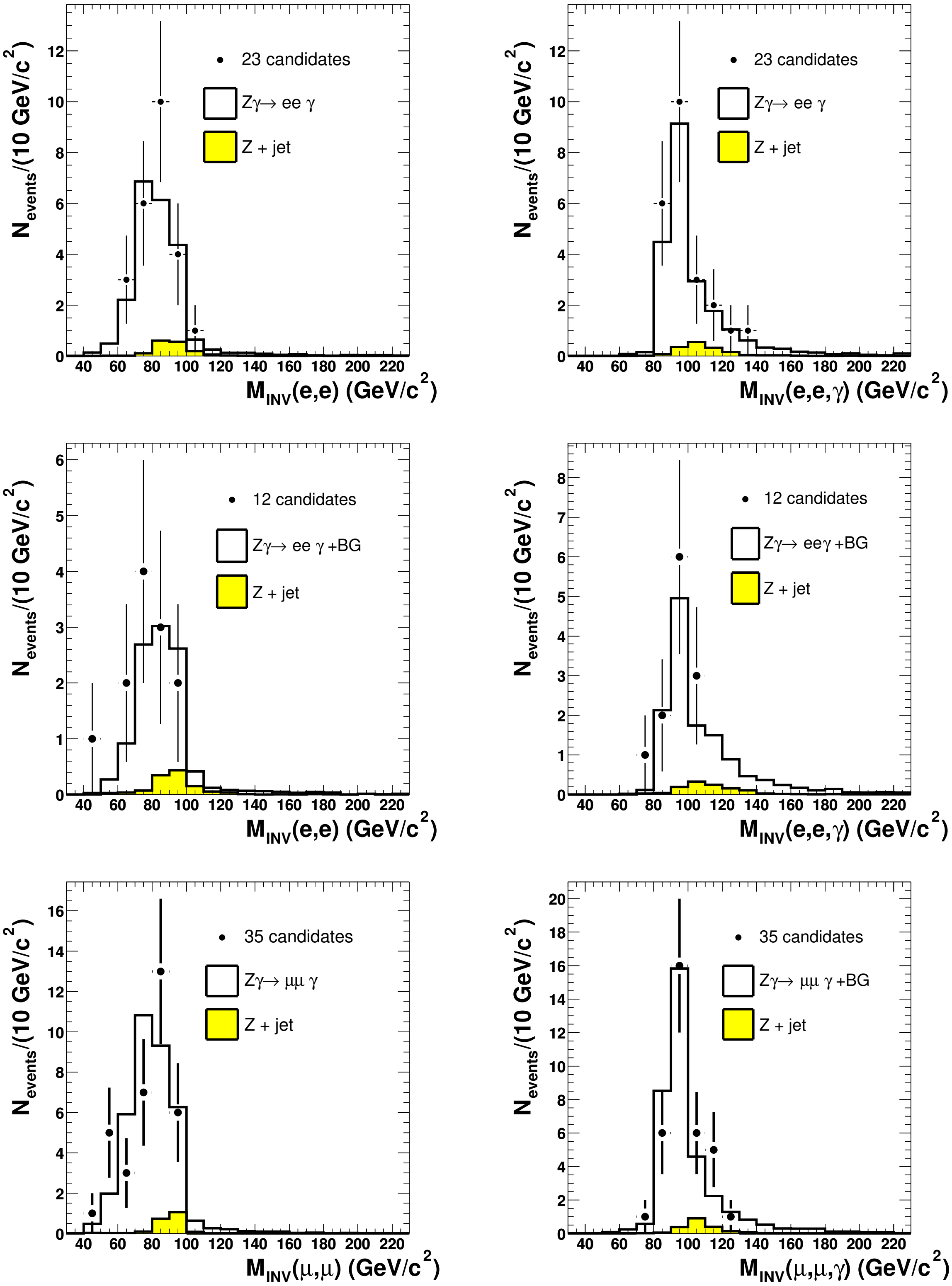

Figure 9: Di-lepton (left) and 3-body ($ll\gamma$) (right) invariant mass for CC $Z \to ee$ (top), CP $Z \to ee$ (middle) and $Z \to \mu\mu$ candidates. The points are the data, the open histogram the Standard Model expectation and the shaded histogram is the estimated QCD background.

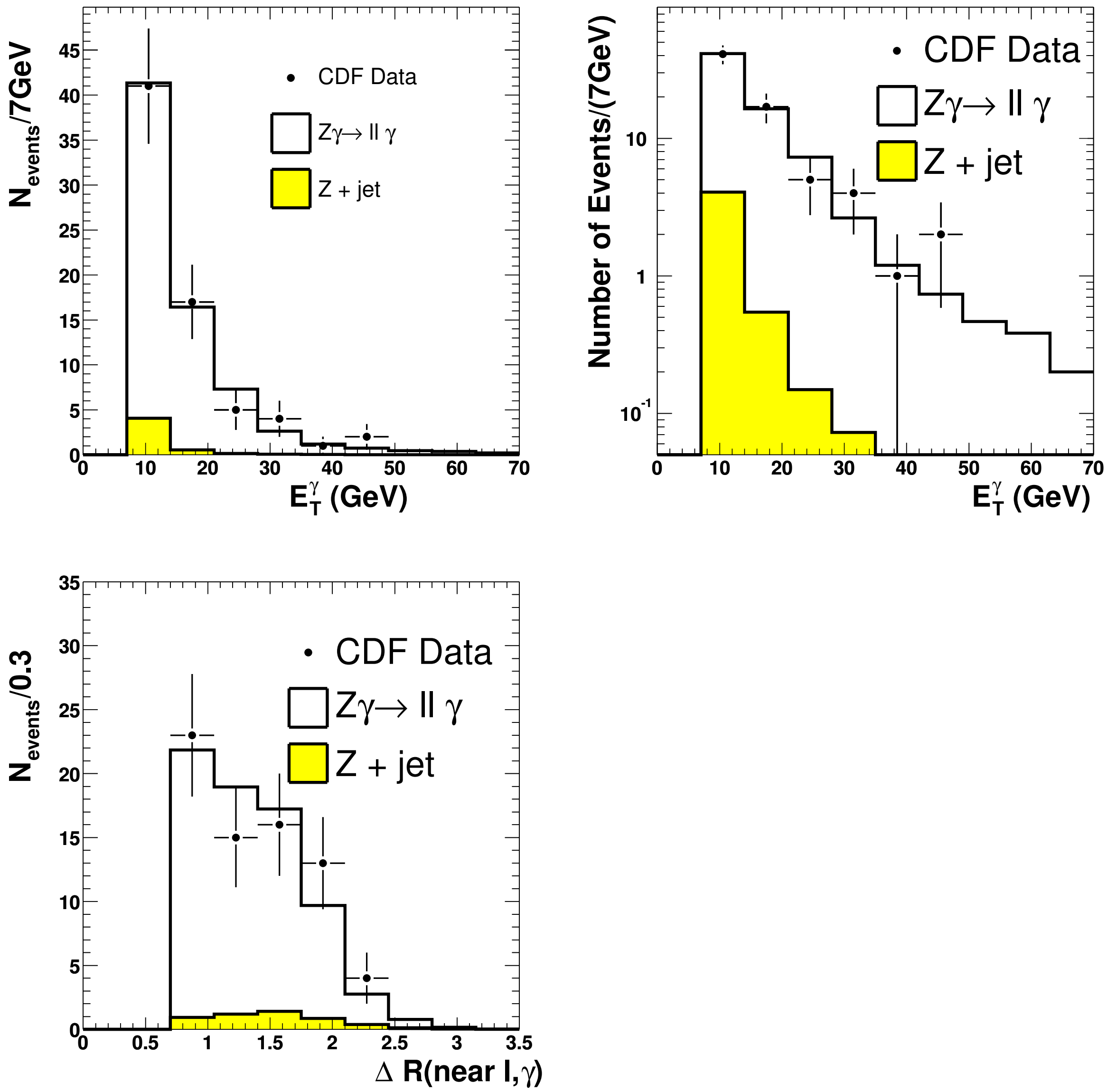

Figure 10: Several distributions for $Z\gamma$ candidates summing the electron and muon channels. The points are the data, the open histogram the Standard Model expectation and the shaded histogram is the estimated QCD background.

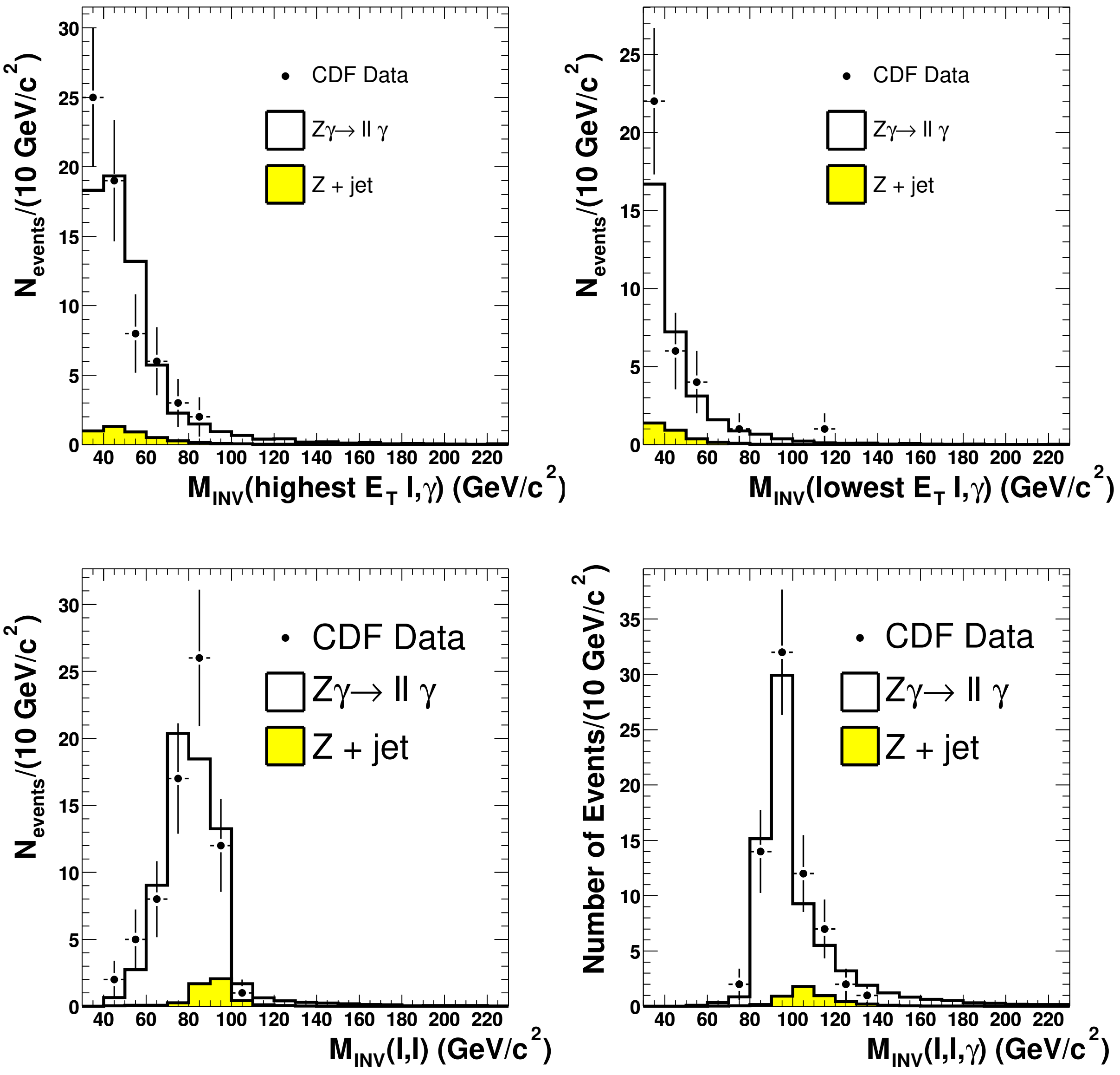

Figure 11: Several distributions for $Z\gamma$ candidates summing the electron and muon channels. The points are the data, the open histograms the full Standard Model expectation and the shaded histogram is the estimated QCD background.

Table 20: Observed and expected numbers of events for $Z\gamma \rightarrow ee\gamma$ and $Z\gamma \rightarrow \mu\mu\gamma$ production.

	Number of Events	
	$Z\gamma \rightarrow e^+e^-\gamma$	$Z\gamma \rightarrow \mu^+\mu^-\gamma$
$Z+\gamma$	31.3 ± 1.6	33.6 ± 1.5
Z+jet fakes	2.8 ± 0.9	2.1 ± 0.6
total SM+BG	34.1 ± 1.8	35.7 ± 1.7
Data	36	35

Table 21: Numbers of events in data and expected for $Z\gamma$ combining the electron and muon channels.

	Number of Events
$Z+\gamma$	64.8 ± 2.6
Z+jet fakes	4.9 ± 1.5
total SM+BG	69.8 ± 3.0
Data	71

now a priori. But, e.g. for $E_t > 70$ GeV 0.7 events are expected and for $E_t^\gamma > 100$ GeV about 0.4 events are expected. For $m(l,l,\gamma) > 300$ GeV about 0.1 events are expected. In this sense we conclude that the event is consistent with the background estimates and more data will be needed to see whether there is any anomalous production. An event display and the exact kinematics will be included in the note asap.

Figure 13 shows the correlation between the dilepton mass and the invariant mass of the $ll\gamma$ system. The events due to FSR off the lepton lines are clustered at values of $M(ll) < 90$ GeV and $M(ll\gamma) \approx 90$ GeV whilst the events from the quark radiation diagram are clustered at $M(ll) \approx 90$ GeV and $M(ll\gamma) > 90$ GeV. The events are consistent with the Z mass in one of the two masses.

8.3 $W\gamma$ and $Z\gamma$ Cross Sections

We extract the cross section for $W\gamma$ production in the kinematic range $\Delta R > 0.7$ and $E_T^\gamma > 7$. The cross section is given by

$$\sigma = \frac{N_{Data} - N_{BG}}{\mathcal{L} \cdot A \cdot \epsilon_{MC} \cdot \epsilon_{corr}}, \tag{1}$$

where N_{Data} is the number of observed events, N_{BG} the number of background events, A the acceptance for this kinematic range and ϵ_{MC} the efficiency in MC and ϵ_{corr} the correction to reproduce the data efficiency (see Section 5).

With $N^{exp}_{W\gamma MC} = \mathcal{L} \cdot \sigma^{MC}_{default} \cdot A \cdot \epsilon_{MC}\epsilon_{corr}$ being the expected number of $W\gamma$ events this simplifies to

$$\sigma = \frac{N_{Data} - N_{BG}}{N^{exp}_{W\gamma MC}} \cdot \sigma^{MC}_{default} \tag{2}$$

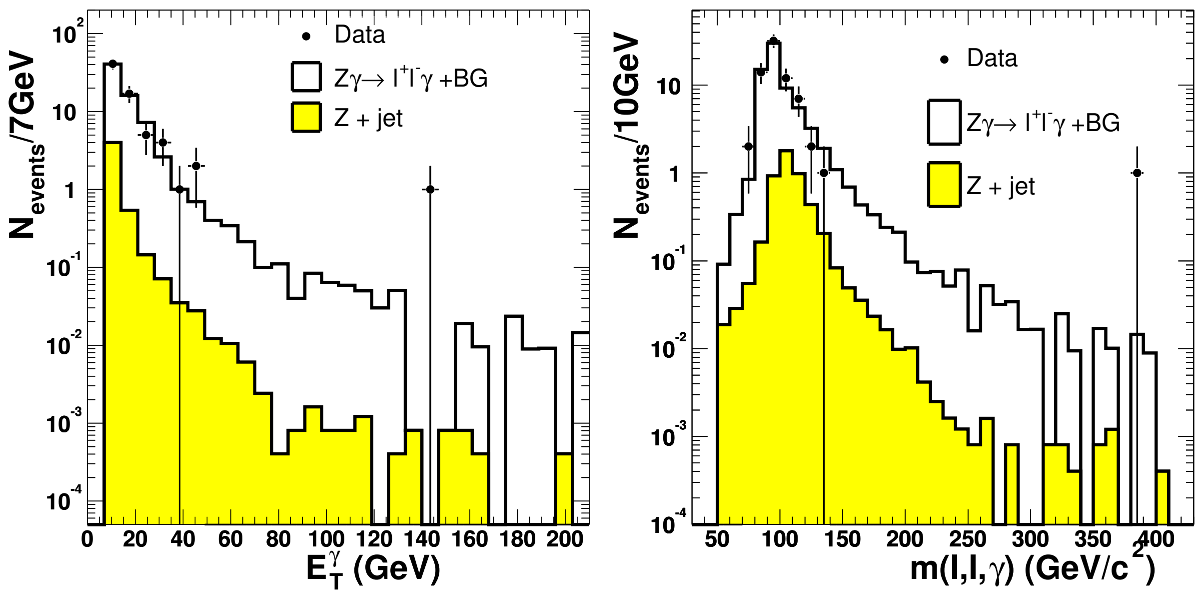

Figure 12: Photon Et and invariant mass distribution for all evbents up to the highest Et and mass values.

for the kinematic range of the `WGAMMA` MC. In order to correct to the kinematic range of the measurement we can simply scale this by the ratio of the theoretical cross section in the two kinematic regions:

$$\frac{\sigma^{MC}_{E_T>7GeV,\Delta R>0.7}}{\sigma^{MC}_{default}} = \frac{19.3 \text{ pb}}{44.7 \text{ pb}} = 0.432 \tag{3}$$

Thus the cross section in the kinematic range $\Delta R > 0.7$ and $E_T^\gamma > 7$ GeV is given simply by

$$\sigma = \frac{N_{Data} - N_{BG}}{N^{exp}_{W\gamma MC}} \cdot \sigma^{MC}_{default} \cdot \frac{\sigma^{MC}_{E_T>7GeV,\Delta R>0.7}}{\sigma^{MC}_{default}} = \frac{N_{Data} - N_{BG}}{N^{exp}_{W\gamma MC}} \cdot \sigma^{MC}_{E_T>7GeV,\Delta R>0.7}. \tag{4}$$

The cross sections results for $W\gamma$ are

$$\begin{aligned} CEM : W\gamma \to e\nu\gamma : \sigma \times BR &= 20.1 \pm 2.6(\text{stat.}) \pm 2.7(\text{syst.}) \pm 1.3(\text{lum.}) \text{ pb} \\ PEM : W\gamma \to e\nu\gamma : \sigma \times BR &= 18.4 \pm 3.8(\text{stat.}) \pm 3.4(\text{syst.}) \pm 1.1(\text{lum.}) \text{ pb} \\ CMUP : W\gamma \to \mu\nu\gamma : \sigma \times BR &= 18.8 \pm 2.9(\text{stat.}) \pm 1.8(\text{syst.}) \pm 1.4(\text{lum.}) \text{ pb} \\ CMX : W\gamma \to \mu\nu\gamma : \sigma \times BR &= 11.5 \pm 3.6(\text{stat.}) \pm 1.8(\text{syst.}) \pm 0.9(\text{lum.}) \text{ pb} \end{aligned} \tag{5}$$

resulting in an average cross section from the CEM, PEM, CMUP, and CMX of $\sigma \times BR = 18.1 \pm 1.6(\text{stat.}) \pm 2.4(\text{syst.}) \pm 1.2(\text{lum.})$ pb compared to a SM expectation of $19.3 \pm 1.4(\text{th.})$ pb. The correlations within the systematics errors and fully taken into account when combining the results. The measured cross section is consistent with the Standard Model expectation.

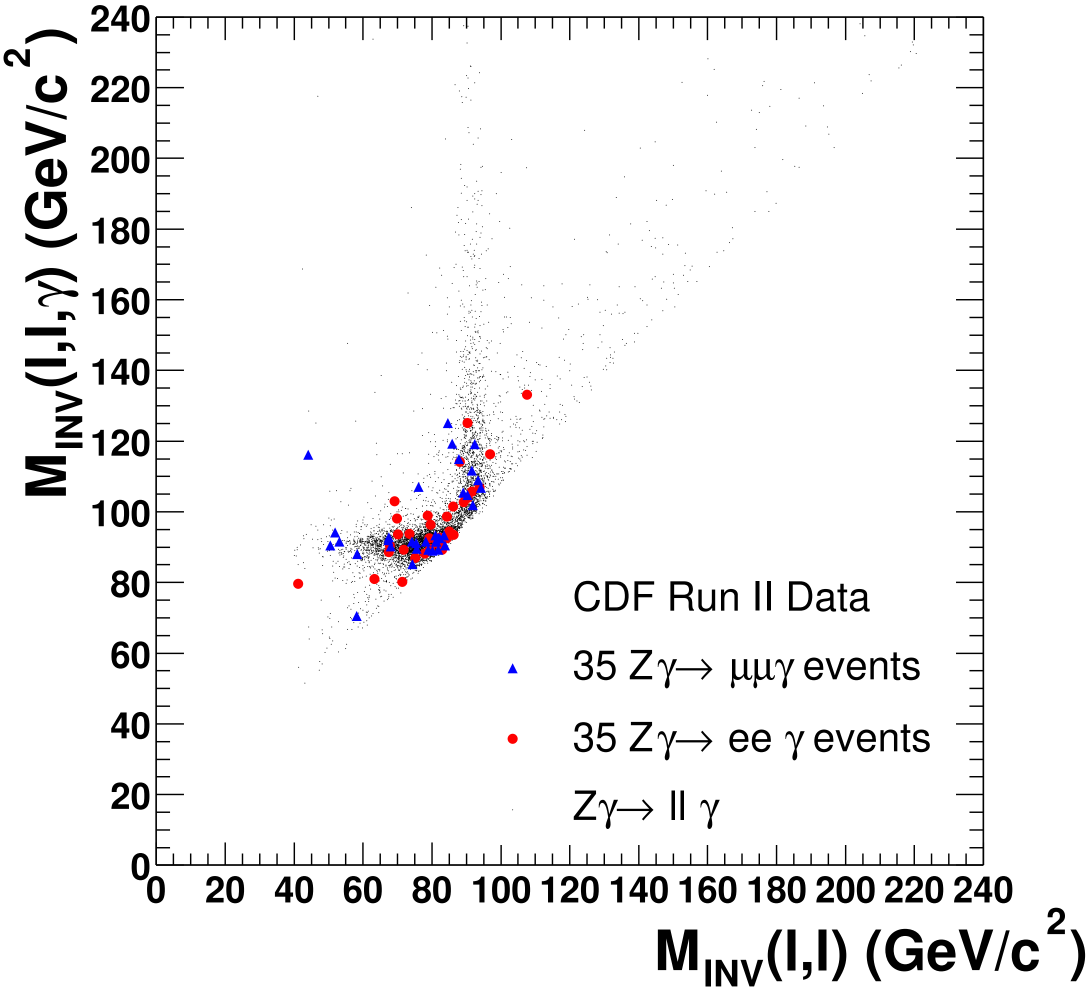

Figure 13: Invariant mass of the two leptons and the photon versus the di-lepton invariant mass for $Z\gamma$ candidates in the electron (red points) and muon (blue points) channel. The black points show the expectation from the $Z\gamma$ MC.

We follow the same procedure for extracting the the $Z\gamma$ cross section. The scale factor for the difference in kinematic range between the MC and the range where the cross section is quoted in this case is:

$$\frac{\sigma^{MC}_{E_T>7GeV,\Delta R>0.7}}{\sigma^{MC}_{default}} = \frac{4.53}{11.7} = 0.387. \tag{6}$$

Using this we obtain the following consistent results for the $Z\gamma$ cross section:

$$\begin{aligned} Z\gamma \to ee\gamma : \sigma \times BR &= 4.8 \pm 0.8(\text{stat.}) \pm 0.3(\text{sys.}) \pm 0.3(\text{lumi})\ \text{pb} \\ Z\gamma \to \mu\mu\gamma : \sigma \times BR &= 4.4 \pm 0.8 \pm 0.2(\text{sys.}) \pm 0.3(\text{lumi})\ \text{pb} \end{aligned} \tag{7}$$

resulting in a combined cross section of $\sigma(Z\gamma) \times BR(Z \to ll) = 4.6 \pm 0.5(\text{stat.}) \pm 0.2(\text{sys.}) \pm 0.3(\text{lumi})$ pb compared to the theoretical prediction of $4.53 \pm 0.32(\text{th.})$ pb. In this measurement the dominant sources of systematic error are the photon ID efficiency and the acceptance uncertainty.

The statistical errors were calculated using the prescription in [28]. Since the asymmetry in the statistical errors was small we symmetrizes the error taking the larger value of the two.

9 Radiation Amplitude Zero

$W\gamma$ production is a special interest due to the presence of a zero in the amplitude of the parton-level subprocesses which contribute to lowest order in the SM of electroweak interactions [29]. For $u\bar{d} \to W^+\gamma (d\bar{u} \to W^-\gamma)$ all contributing helicity amplitudes vanish for $cos\theta^* = -1/3(+1/3)$, where θ^* is the angle between the quark and the photon in the parton center-of-mass frame, it's because t- and u-channel diagrams interfere destructively to s-channel diagram.

In practice, however, this zero is difficult to observe. Higher-order QCD corrections [9, 30] and finite W width effects, together with photon radiation from the final state lepton line, tend to fill in this dip [31]. Finally, finite detector resolution effects and ambiguities in reconstructing the parton center-of-mass frame represent an additional major complication in the extraction of the $cos\theta^*$. The ambiguities are associated with the non-observation of the neutrino arising from W decay.

However, it has been suggested that this could be observed in the difference in pseudorapidity between the lepton and the photon, $\Delta\eta = \eta_l - \eta_\gamma$, originating from the W decay as tools to observe the radiation zero in $p\bar{p} \to W\gamma$ [32]. In this section we discuss the $\Delta\eta$ distribution. This phenomenon has never been observed experimentally and is not present in $Z\gamma$ production due to the absence of the s-channel diagram.

To suppress final state lepton radiation we apply a cut on the cluster transverse mass of 90 GeV. Figure 9 shows $\Delta\eta \cdot Q_l$ for the CMUP, CMX and combined muon sample and the central electron sample where Q_l is the charge of the lepton. The combined plot of the electron and muon channels is shown in Figure 9.

Figure 9 shows the $\Delta\eta \cdot Q_l$ distribution for the $Z\gamma$ candidates. Note, that every event has two entries (one for each lepton) in this plot. The data are in good agreement with the SM expectation. The distribution peaks at $|\Delta\eta| \approx 0$ and is symmetric around 0.

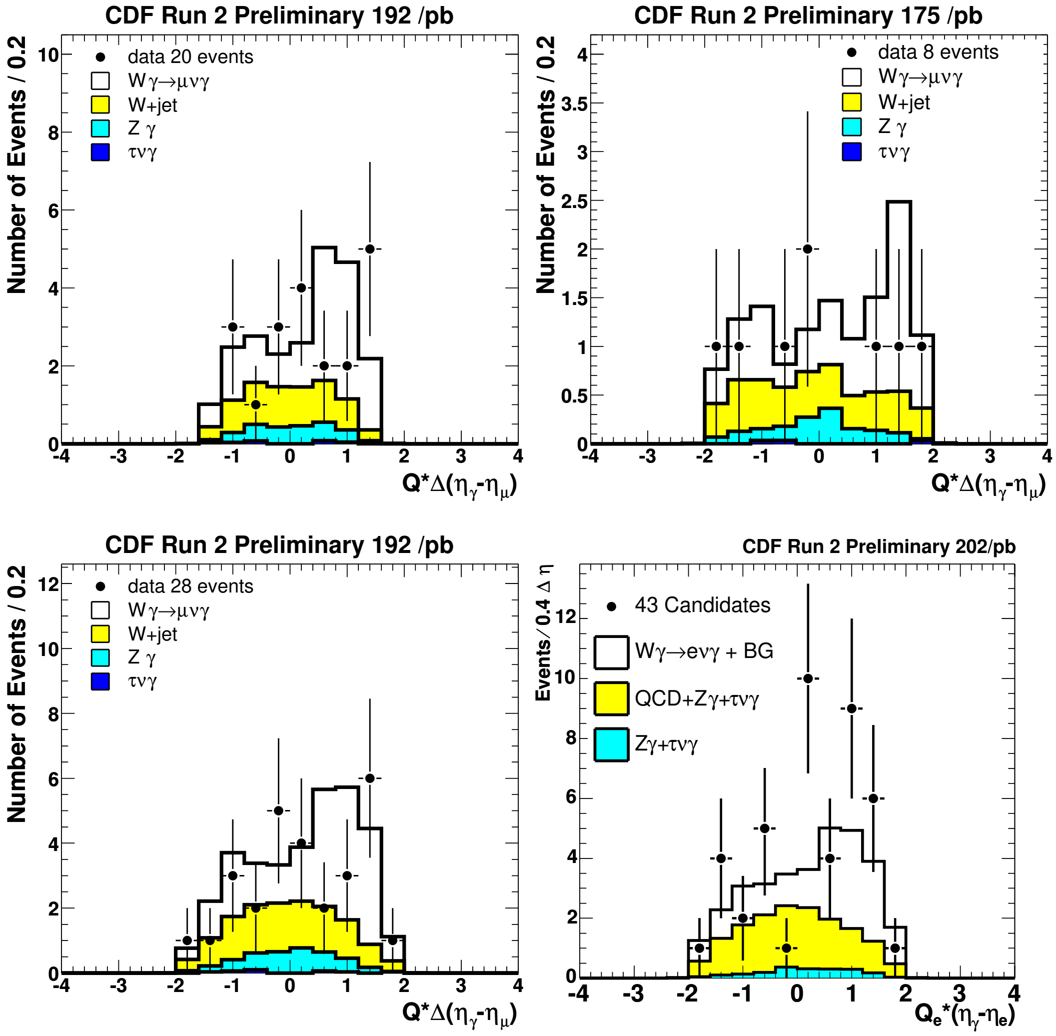

Figure 14: $\Delta\eta \cdot Q_l$ for $W\gamma \to \mu\nu\gamma$ candidates with CMUP, CMX (upper left and right) and all CMUP + CMX (lower left) and $W\gamma \to e\nu\gamma$ candidates with central electron (lower right) compared to the Standard Model expectation.

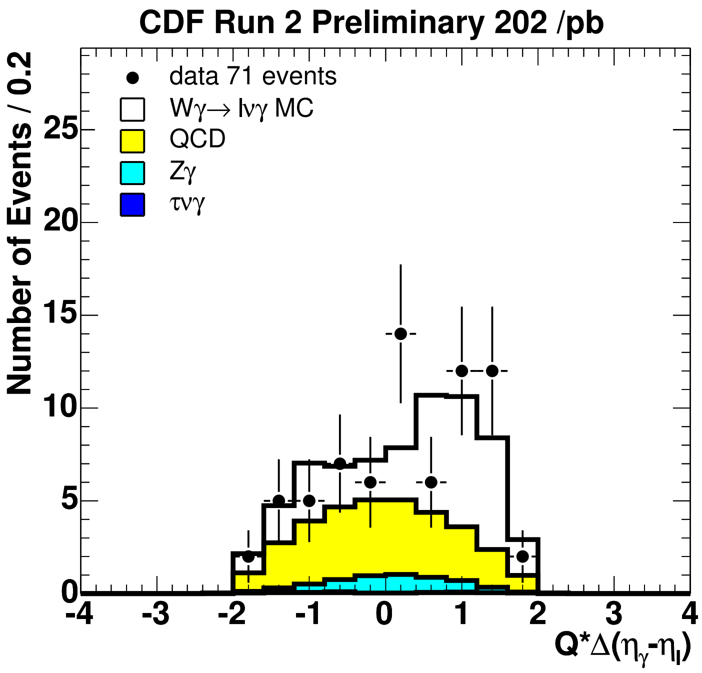

Figure 15: $\Delta\eta \cdot Q_l$ for the combined central $W \to e\nu$ and $W \to \mu\nu$ candidates.

The data are in good agreement with the Standard Model expectation and further studies are needed to conclude on whether or not the RAZ has been observed or with which luminosity an observation is possible. Note, that the QCD background is rather large at high cluster transverse mass and that it tends to fill in the $\Delta\eta$ distribution where one hopes to observe the RAZ. A further suppression of this background is desirable for this analysis.

10 Conclusions

We have presented a measurement of the $W\gamma$ and $Z\gamma$ production cross sections at $\sqrt{s} = 1.96$ TeV. We have used all available leptons triggers (central and plug calorimeters, CMX and CMUP muons) to select W and Z candidates inclusively and then selected an additional photon.

We have presented a cross section measurement in the kinematic range $\Delta R_{l\gamma} > 0.7$ and $E_t^\gamma > 7$ GeV and measured several kinematic distributions. The results are in excellent agreement with the Standard Model expectations.

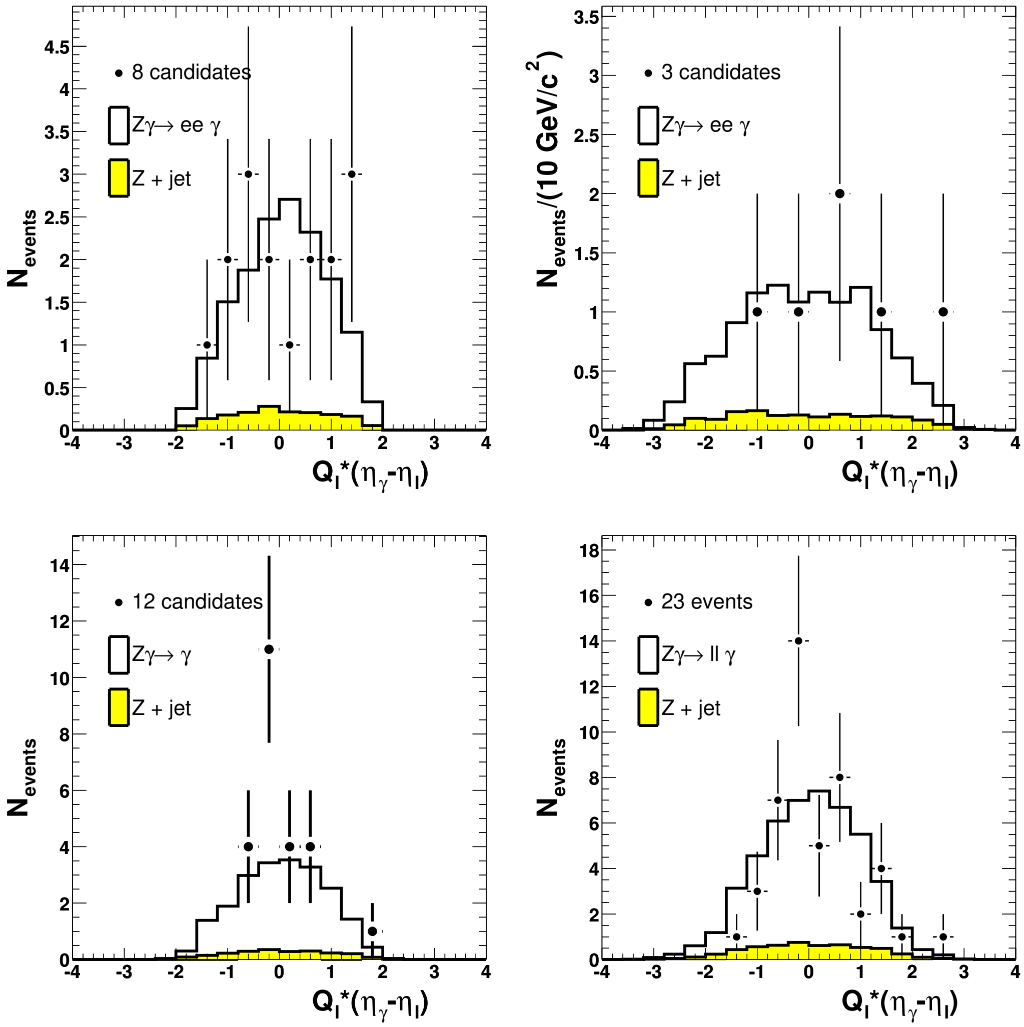

Figure 16: $\Delta\eta \cdot Q_l$ for CC, CP, $\mu\mu$ and all $Z\gamma \to ll\gamma$ candidates (points) compared to the Standard Model expectation.

APPENDIX

A Expectations of the number of events

We calculate the number of the signal $W\gamma$ expectation of CMUP muon is,

$$N_{W\gamma}^{CMUP} = (A \times e_{W\gamma}) \cdot \sigma_{W\gamma}^{E_T>5,\Delta R>0.2} \cdot \epsilon_{trig}^{CMUP} \cdot \epsilon_{ID}^{CMUP} \cdot \epsilon_{rec}^{CMUP} \cdot \epsilon_{conv} \cdot \epsilon_{z0} \cdot \epsilon_{cos} \cdot \int \mathcal{L}dt, \quad (8)$$

where $A \times e_{W\gamma}$ is the acceptance times efficiency estimated with the `WGAMMA` Monte Carlo.

B Definition of $W/Z\gamma$ cross section

The definition of $W/Z\gamma$ cross section detailed in Section 8.3 are,

$$\sigma(W\gamma) = \frac{(N_{Data} - N_{QCD} - N_{Z\gamma} - N_{\tau}) \times \sigma_{W\gamma,NLO}^{E_T>7,\Delta R>0.7}}{N_{W\gamma}} \quad (9)$$

$$\sigma(Z\gamma) = \frac{(N_{Data} - N_{QCD}) \times \sigma_{Z\gamma,NLO}^{E_T>7,\Delta R>0.7}}{N_{Z\gamma}} \quad (10)$$

C Statistical error of the number of $W\gamma$ expectations

C.1 Statistical error of the SM $W\gamma$ CMUP

The statistical error of $N_{w\gamma}$, the number of the signal expectation of $W\gamma$, comes from the statistics of the `WGAMMA` Monte Carlo. In our case, statistical error appears in $A \times e_{W\gamma}$ in Eq.(8).

$$\delta(N_{W\gamma}^{CMUP}) = \sqrt{(A \times e_{W\gamma}) \times (1 - A \times e_{W\gamma})/N_{Gen}^{|Z_0|<60cm}} \times \sigma_{W\gamma}^{E_T>5,\Delta R>0.2} \cdot \epsilon_i \ldots \int \mathcal{L}dt. \quad (11)$$

Note that due to the difficulty of estimating z-vertex correction factor (data/mc) for the plug `WGAMMA` MC, we applied $|z0|$ <60 cm cut at first. We define $A \times e_{W\gamma}$ as

$$\frac{\text{pass all } W\gamma \text{ requirement with WGAMMA MC}}{\text{number of generated events which pass } |z_0| < 60cm \text{ cut with WGAMMA MC}} \quad (12)$$

C.2 Combine the statistical error of CMUP and CMX

As the statistical error of CMUP doesn't correlate to that of CMX,

$$\delta(N_{W\gamma}^{CMUPX}) = \sqrt{\delta(N_{W\gamma}^{CMUP})^2 + \delta(N_{W\gamma}^{CMX})^2} \quad (13)$$

C.3 Statistical error of the total SM expectation

As each of statistical error doesn't correlate, we can define it with folowing equation,

$$\delta(N_{tot}^{CMUPX}) = \sqrt{\delta(N_{W\gamma}^{CMUPX})^2 + \delta(N_{Z\gamma}^{CMUPX})^2 + \delta(N_{\tau}^{CMUPX})^2}. \tag{14}$$

D Systematic error of $W\gamma$

D.1 Systematic error of the SM $W\gamma$ CMUP

$$\delta N_{W\gamma}^{CMUP} = N_{W\gamma}^{CMUP} \times \sqrt{\delta(\epsilon_a)^2 + \delta(\epsilon_b)^2 + \dots} \tag{15}$$

D.2 Combinning of the systematic error of $W\gamma$ CMUP + CMX

I categorize the systematic uncertainties for a convenience.

ϵ^{μ} Efficiencies (or correction factors) which are common to CMUP and CMX

ϵ^{CMUP} Efficiencies (or correction factors) for CMUP muons

ϵ^{CMX} Efficiencies (or correction factors) for CMX muons.

The SM $W\gamma$ expectation, $N_{W\gamma}$, combining CMUP and CMX channel is,

$$\begin{aligned} N_{W\gamma}^{CMUPX} &= N_{W\gamma}^{CMUP} + N_{W\gamma}^{CMX} \\ &= \sigma \cdot (A \times e_{W\gamma}^{CMUP}) \cdot \epsilon^{CMUPX} \cdot \epsilon^{CMUP} \cdot \int \mathcal{L}^{CMUP} dt \\ &+ \sigma \cdot (A \times e_{W\gamma}^{CMX}) \cdot \epsilon^{CMUPX} \cdot \epsilon^{CMX} \cdot \int \mathcal{L}^{CMX} dt \end{aligned} \tag{16}$$

where,

$$\sigma = \sigma_{W\gamma}^{E_T>5, \Delta R>0.2} \tag{17}$$

$$\epsilon^{CMUPX} = \epsilon_{conv} \cdot \epsilon_{z0} \cdot \epsilon_{cos} \cdot \epsilon_{COT} (\cdot \epsilon_{ID}^{\gamma} \cdot \epsilon_{\mu scale} \cdot \epsilon_{\gamma scale} \cdot \epsilon_{acc}) \tag{18}$$

$$\epsilon^{CMUP} = \epsilon_{rec}^{CMUP} \cdot \epsilon_{ID}^{CMUP} \cdot \epsilon_{trig}^{CMUP} \tag{19}$$

$$\epsilon^{CMX} = \epsilon_{rec}^{CMX} \cdot \epsilon_{ID}^{CMX} \cdot \epsilon_{trig}^{CMX}. \tag{20}$$

These factors, $\epsilon_{ID}^{\gamma} \cdot \epsilon_{\mu scale} \cdot \epsilon_{\gamma scale} \cdot \epsilon_{acc}$ are included in $A \times e_{W\gamma}$, but I include their systematic errors to ϵ^{CMUPX} just to make error calculation easier.

$$\begin{aligned} \delta(N_{W\gamma}^{CMUPX})^2 = &\left(\frac{\partial N_{W\gamma}^{CMUPX}}{\partial \epsilon^{CMUPX}}\right)^2 \delta(\epsilon^{CMUPX})^2 + \left(\frac{\partial N_{W\gamma}^{CMUPX}}{\partial \epsilon^{CMUP}}\right)^2 \delta(\epsilon^{CMUP})^2 \\ &+ \left(\frac{\partial N_{W\gamma}^{CMUPX}}{\partial \epsilon^{CMX}}\right)^2 \delta(\epsilon^{CMX})^2 \\ &= (N_{W\gamma}^{CMUPX})^2 \left(\frac{\delta \epsilon^{CMUPX}}{\epsilon^{CMUPX}}\right)^2 + (N_{W\gamma}^{CMUP})^2 \left(\frac{\delta \epsilon^{CMUP}}{\epsilon^{CMUP}}\right)^2 + (N_{W\gamma}^{CMX})^2 \left(\frac{\delta \epsilon^{CMX}}{\epsilon^{CMX}}\right)^2 \end{aligned} \tag{21}$$

where,

$$
\begin{aligned}
\left(\frac{\delta\epsilon^{CMUPX}}{\epsilon^{CMUPX}}\right)^2 = &\left(\frac{\delta\epsilon_{conv}}{\epsilon_{conv}}\right)^2 + \left(\frac{\delta\epsilon_{z0}}{\epsilon_{z0}}\right)^2 + \left(\frac{\delta\epsilon_{cos}}{\epsilon_{cos}}\right)^2 + \left(\frac{\delta\epsilon_{COT}}{\epsilon_{COT}}\right)^2 \\
&+ \left(\frac{\delta\epsilon^{\gamma}_{ID}}{\epsilon^{\gamma}_{ID}}\right)^2 + \left(\frac{\delta\epsilon_{\mu scale}}{\epsilon_{\mu scale}}\right)^2 + \left(\frac{\delta\epsilon_{\gamma scale}}{\epsilon_{\gamma scale}}\right)^2 + \left(\frac{\delta\epsilon_{acc}}{\epsilon_{acc}}\right)^2
\end{aligned} \tag{22}
$$

$$
\left(\frac{\delta\epsilon^{CMUP}}{\epsilon^{CMUP}}\right)^2 = \left(\frac{\delta\epsilon^{CMUP}_{rec}}{\epsilon^{CMUP}_{rec}}\right)^2 + \left(\frac{\delta\epsilon^{CMUP}_{ID}}{\epsilon^{CMUP}_{ID}}\right)^2 + \left(\frac{\delta\epsilon^{CMUP}_{trig}}{\epsilon^{CMUP}_{trig}}\right)^2 \tag{23}
$$

$$
\left(\frac{\delta\epsilon^{CMX}}{\epsilon^{CMX}}\right)^2 = \left(\frac{\delta\epsilon^{CMX}_{rec}}{\epsilon^{CMX}_{rec}}\right)^2 + \left(\frac{\delta\epsilon^{CMX}_{ID}}{\epsilon^{CMX}_{ID}}\right)^2 + \left(\frac{\delta\epsilon^{CMX}_{trig}}{\epsilon^{CMX}_{trig}}\right)^2 \tag{24}
$$

D.3 Systematic error of total SM expectation : μ channel

The total SM expectation, N^{CMUPX}_{tot}, that is combining $W\gamma$ SM model expectation and their background for CMUP and CMX channel is,

$$
\begin{aligned}
N^{CMUPX}_{tot} &= N^{CMUP}_{W\gamma} + N^{CMX}_{W\gamma} \\
&+ N^{CMUPX}_{QCD} \\
&+ N^{CMUP}_{Z\gamma} + N^{CMX}_{Z\gamma} \\
&+ N^{CMUP}_{\tau} + N^{CMX}_{\tau}
\end{aligned} \tag{25}
$$

then $\delta(N^{CMUPX}_{tot})$ is,

$$
\begin{aligned}
\delta(N^{CMUPX}_{tot})^2 = &\left(\frac{\partial N^{CMUPX}_{tot}}{\partial\epsilon^{CMUPX}}\right)^2 \delta(\epsilon^{CMUPX})^2 + \left(\frac{\partial N^{CMUPX}_{tot}}{\partial\epsilon^{CMUP}}\right)^2 \delta(\epsilon^{CMUP})^2 \\
&+ \left(\frac{\partial N^{CMUPX}_{tot}}{\partial\epsilon^{CMX}}\right)^2 \delta(\epsilon^{CMX})^2 + \left(\frac{\partial N^{CMUPX}_{tot}}{\partial N^{CMUPX}_{QCD}}\right)^2 \delta(N^{CMUPX}_{QCD})^2 \\
&= (N^{CMUPX}_{tot})^2 \left(\frac{\delta\epsilon^{CMUPX}}{\epsilon^{CMUPX}}\right)^2 + (N^{CMUP}_{W\gamma})^2 \left(\frac{\delta\epsilon^{CMUP}}{\epsilon^{CMUP}}\right)^2 \\
&+ (N^{CMX}_{W\gamma})^2 \left(\frac{\delta\epsilon^{CMX}}{\epsilon^{CMX}}\right)^2 + \delta(N^{CMUPX}_{QCD})^2
\end{aligned} \tag{26}
$$

D.4 Systematic error of total SM expectation : $e + \mu$ channel

To combine electron and muon channel, we can categorize their systematic unsertainties into : $\epsilon^{e\mu}, \epsilon^{e}, \epsilon^{c}$(central electron), ϵ^{p}(plug electron), $\epsilon^{\mu}, \epsilon^{CMUP}, \epsilon^{CMX}$, and $\epsilon^{c\mu}$(central electron and muon). The systematic error of total SM expectation ($\delta(N_{e\mu})$) is,

$$\begin{aligned}
\delta(N_{e\mu})^2 = (N^{e\mu}_{tot})^2 \left(\frac{\delta\epsilon^{e\mu}}{\epsilon^{e\mu}}\right)^2 + (N^{e}_{tot})^2 \left(\frac{\delta\epsilon^{e}}{\epsilon^{e}}\right)^2 \\
+ (N^{c}_{tot})^2 \left(\frac{\delta\epsilon^{c}}{\epsilon^{c}}\right)^2 + (N^{p}_{tot})^2 \left(\frac{\delta\epsilon^{p}}{\epsilon^{p}}\right)^2 \\
+ (N^{\mu}_{tot})^2 \left(\frac{\delta\epsilon^{\mu}}{\epsilon^{\mu}}\right)^2 + (N^{CMUP}_{tot})^2 \left(\frac{\delta\epsilon^{CMUP}}{\epsilon^{CMUP}}\right)^2 \\
+ (N^{CMX}_{tot})^2 \left(\frac{\delta\epsilon^{CMX}}{\epsilon^{CMX}}\right)^2 + (N^{c\mu}_{tot})^2 \left(\frac{\delta\epsilon^{c\mu}}{\epsilon^{c\mu}}\right)^2 + \delta(N^{tot}_{QCD})^2
\end{aligned} \tag{27}$$

E Systematic error of $Z\gamma$

I have different correlations to the wg. ie some of my errors are correlated between the cc and cp, or between cmup and cmx, or between all channels.

If i class the different errors into groups, ie, δ^{cc}_{sys}, δ^{cp}_{sys}, δ^{cccp}_{sys}, δ^{cmup}_{sys}, δ^{cmx}_{sys}, δ^{cmupx}_{sys}, δ^{all}_{sys}.

$$\begin{aligned}
(\delta_{sys}(N_{Z\gamma}))^2 &= (N^{cc}_{Z\gamma}\delta^{cc}_{sys})^2 + (N^{cp}_{Z\gamma}\delta^{cp}_{sys})^2 + (N^{cccp}_{Z\gamma}\delta^{cccp}_{sys})^2 \\
&\quad +(N^{cmup}_{Z\gamma}\delta^{cmup}_{sys})^2 + (N^{cmx}_{Z\gamma}\delta^{cmx}_{sys})^2 + (N^{cmupx}_{Z\gamma}\delta^{cmupx}_{sys})^2 \\
&\quad +(N^{all}_{Z\gamma}\delta^{all}_{sys})^2
\end{aligned}$$

where, $N^{cccp}_{Z\gamma}$ is the number of cc and cp events.

F Statistical error of $W\gamma$ cross section

The statistical error of $\sigma(W\gamma)$ is coming from only the number of data. I assume Eq(9) as

$$\sigma(W\gamma) = \alpha \cdot (N_{DATA} - N_{BG}) \tag{28}$$

where,

$$\alpha = \frac{\sigma^{E_T>7,\Delta R>0.7}_{W\gamma,NLO}}{N_{W\gamma}}. \tag{29}$$

then,

$$\begin{aligned}
\delta(\sigma(W\gamma)) &= \frac{\partial\sigma(W\gamma)}{\partial(N_{DATA})} \cdot \delta(N_{DATA}) \\
&= \alpha \cdot \delta(N_{DATA}) \\
&= \frac{\sqrt{N_{DATA}} \cdot \sigma^{E_T>7,\Delta R>0.7}_{W\gamma,NLO}}{N_{W\gamma}}.
\end{aligned} \tag{30}$$

To get above result, I used these relations.

$$\frac{\partial\sigma(W\gamma)}{\partial N_{DATA}} = \alpha, \quad \delta(N_{Data}) = \sqrt{N_{Data}}. \tag{31}$$

G Systematic error of the cross section

The systematic error of the cross section have two components, statistics of the Monte Carlo and pure systematic uncertainties.

$$\delta(\sigma(W\gamma)) = \sqrt{\delta(\sigma^{MC}(W\gamma))^2 + \delta(\sigma^{puresys}(W\gamma))^2} \tag{32}$$

As N_{BG} and $N_{W\gamma}$ in Eq(9) have both systematics, I will show a partial differenciation for a one case.

$$\delta(\sigma(W\gamma))^2 = \left(\frac{\partial\sigma(W\gamma)}{\partial N_{BG}}\right)^2 \delta(N_{BG})^2 + \left(\frac{\partial\sigma(W\gamma)}{\partial N_{W\gamma}}\right)^2 \delta(N_{W\gamma})^2 \tag{33}$$

Here, using these equations,

$$\begin{aligned} \frac{\partial\sigma(W\gamma)}{\partial N_{BG}} &= -\frac{\sigma^{E_T>7,\Delta R>0.7}_{W\gamma,NLO}}{N_{W\gamma}} \\ \frac{\partial\sigma(W\gamma)}{\partial N_{W\gamma}} &= -\frac{(N_{Data} - N_{BG}) \cdot \sigma^{E_T>7,\Delta R>0.7}_{W\gamma,NLO}}{(N_{W\gamma})^2} \end{aligned} \tag{34}$$

The result is

$$\begin{aligned} \delta(\sigma(W\gamma))^2 &= \left(\frac{\sigma^{E_T>7,\Delta R>0.7}_{W\gamma,NLO}}{N_{W\gamma}}\right)^2 \cdot \delta(N_{BG})^2 \\ &\quad + \left(\frac{(N_{Data} - N_{BG}) \cdot \sigma^{E_T>7,\Delta R>0.7}_{W\gamma,NLO}}{(N_{W\gamma})^2}\right)^2 \cdot \delta(N_{W\gamma})^2 \\ &= \left(\frac{\sigma^{E_T>7,\Delta R>0.7}_{W\gamma,NLO}}{N_{W\gamma}}\right)^2 \cdot \left(\delta(N_{BG})^2 + \left(\frac{N_{Data} - N_{BG}}{N_{W\gamma}}\right)^2 \cdot \delta(N_{W\gamma})^2\right) \end{aligned} \tag{35}$$

So, $\delta(\sigma^{MC}(W\gamma))^2$ and $\delta(\sigma^{puresys}(W\gamma))^2$ are

$$\begin{aligned} \delta(\sigma^{MC}(W\gamma))^2 &= \left(\frac{\sigma^{E_T>7,\Delta R>0.7}_{W\gamma,NLO}}{N_{W\gamma}}\right)^2 \cdot \left(\delta(N^{MC}_{BG})^2 + \left(\frac{N_{Data} - N_{BG}}{N_{W\gamma}}\right)^2 \cdot \delta(N^{MC}_{W\gamma})^2\right) \\ \delta(\sigma^{puresys}(W\gamma))^2 &= \left(\frac{\sigma^{E_T>7,\Delta R>0.7}_{W\gamma,NLO}}{N_{W\gamma}}\right)^2 \cdot \left(\delta(N^{sys}_{BG})^2 + \left(\frac{N_{Data} - N_{BG}}{N_{W\gamma}}\right)^2 \cdot \delta(N^{sys}_{W\gamma})^2\right) \end{aligned} \tag{36}$$

where, $\delta(N^{MC}_{BG})$ is the statistical error of the $Z\gamma$ and $W\gamma \to \tau\nu\gamma$ MC (see Eq.(11)), and $\delta(N^{sys}_{BG})$ is the systematical error of the backgrounds, W+jet, $Z\gamma$ and $W\gamma \to \tau\nu\gamma$.

H Systematic error due to the luminosity for σ

This error appears in $N_{W\gamma}, N_{Z\gamma}, N_\tau$ in Eq.(9) ;

$$\begin{aligned}
\sigma(W\gamma) &= \frac{(N_{Data} - N_{QCD}) \cdot \sigma^{E_T>7,\Delta R>0.7}_{W\gamma,NLO}}{N_{W\gamma}} - \frac{(N_{Z\gamma} + N_\tau) \cdot \sigma^{E_T>7,\Delta R>0.7}_{W\gamma,NLO}}{N_{W\gamma}} \\
&= \frac{(N_{Data} - N_{QCD}) \cdot \sigma^{E_T>7,\Delta R>0.7}_{W\gamma,NLO}}{C_{W\gamma}} \cdot \frac{1}{L} - \frac{(C_{Z\gamma} + C_\tau) \cdot L \cdot \sigma^{E_T>7,\Delta R>0.7}_{W\gamma,NLO}}{C_{W\gamma} \cdot L},
\end{aligned} \tag{37}$$

where $N_{W\gamma} = C_{W\gamma} \cdot L$, $N_{Z\gamma} = C_{Z\gamma} \cdot L$ and $N_\tau = C_\tau \cdot L$. Then $\delta(\sigma(W\gamma))^2$ is,

$$\begin{aligned}
\delta(\sigma(W\gamma))^2 &= \left(\frac{1}{L^2} \cdot \left(\frac{(N_{Data} - N_{QCD}) \cdot \sigma^{E_T>7,\Delta R>0.7}_{W\gamma,NLO}}{C_{W\gamma}}\right)\right)^2 \cdot \delta L^2 \\
&= \left(\frac{(N_{Data} - N_{QCD}) \cdot \sigma^{E_T>7,\Delta R>0.7}_{W\gamma,NLO}}{N_{W\gamma}}\right)^2 \cdot \left(\frac{\delta L}{L}\right)^2 \\
\delta(\sigma(W\gamma)) &= \left(\frac{(N_{Data} - N_{QCD}) \cdot \sigma^{E_T>7,\Delta R>0.7}_{W\gamma,NLO}}{N_{W\gamma}}\right) \cdot \left(\frac{\delta L}{L}\right).
\end{aligned} \tag{38}$$

where $\delta L/L$ is 6%.

I Propagation of errors

I.1 $N = ab$

If $N = ab$ and error of a and b are $a \pm \delta(a)$, $b \pm \delta(b)$ having this relationship of $\frac{\delta(a)}{a} = A\%$, $\frac{\delta(b)}{b} = B\%$, the error of N ($\delta(N)$) is,

$$\begin{aligned}
\delta(N)^2 &= \left(\frac{\partial N}{\partial a}\right)^2 \delta(a)^2 + \left(\frac{\partial N}{\partial b}\right)^2 \delta(b)^2 \\
&= b^2\delta(a)^2 + a^2\delta(b)^2 \\
&= \frac{N^2\delta(a)^2}{a^2} + \frac{N^2\delta(b)^2}{b^2} \\
&= N^2A^2 + N^2B^2
\end{aligned} \tag{39}$$

$$\delta N = N\sqrt{A^2 + B^2} \tag{40}$$

I.2 $N = ab + ac$

If $N = ab + ac = N_b + N_c$ ($N_b = ab, N_c = ac$) and the error of a, b and c are $a \pm \delta(a)$, $b \pm \delta(b)$ and $c \pm \delta(c)$, and their fraction are $\frac{\delta(a)}{a} = A\%$, $\frac{\delta(b)}{b} = B\%$, and $\frac{\delta(c)}{b} = C\%$. The error of N, $\delta(N)$, is,

$$\begin{aligned}
\delta(N)^2 &= \left(\frac{\partial N}{\partial a}\right)^2 \delta(a)^2 + \left(\frac{\partial N}{\partial b}\right)^2 \delta(b)^2 + \left(\frac{\partial N}{\partial c}\right)^2 \delta(c)^2 \\
&= (b+c)^2\delta(a)^2 + a^2\delta(b)^2 + a^2\delta(c)^2 \\
&= N^2\left(\frac{\delta a}{a}\right)^2 + N_b^2\left(\frac{\delta b}{b}\right)^2 + N_c^2\left(\frac{\delta c}{c}\right)^2 \\
&= N^2 \cdot A^2 + N_b^2 \cdot B^2 + N_c^2 \cdot C^2
\end{aligned} \tag{41}$$

References

[1] LEP EWWG, "A Combination of Preliminary Results on Gauge Boson Couplings Measured by the LEP Experiments", LEPEWWG/TGC/2002-02 (see also `http://lepewwg.web.cern.ch/LEPEWWG/lepww/tgc/`

[2] B. Abbott et al., "Studies of WW and WZ production and limits on anomalous $WW\gamma$ and WWZ couplings", Phys. Rev. D 60, 072002 (1999).

[3] D. Benjamin et al., "Event Selection in CDF Run I $V+\gamma$ Analysis", CDF note 5999.

[4] D. Benjamin et al., "Cross Section Measurements for W+photon and Z+photon Production in Run II", CDF note 6366.

[5] D. Benjamin et al., "Update of the $V+\gamma$ Analysis for summer 2003", CDF note 6601.

[6] http://www-cdf.fnal.gov/internal/dqm/goodrun/good.html

[7] U. Baur and E.L. Berger, "Probing the $WW\gamma$ vertex at the Fermilab Tevatron Collider", Phys. Rev. D **41**, 1476 (1990).

[8] Doug Benjamin, Al Goshaw, Helen Hayward, Beate Heinemann, Michael Kirby, Naho Tanimoto "Theoretical Predictions of W+Gamma and Z+Gamma Production in Run II", CDF note 6619.

[9] U. Baur, T. Han, and J Ohnemus, "QCD corrections to hadronic $W\gamma$ production with nonstandard $WW\gamma$ couplings", Phys. Rev. D **48**, 5140 (1993).

[10] D. Amidei et al., "Measurement of $\sigma \times B(W \to e\nu)$, $\sigma \times B(Z \to ee)$ and the ratio R using CDF Run 2 Data", CDF note 6681.

[11] D. Amidei et al., "Measurement of $W \to \mu\nu$) and $Z \to \mu\mu$ production cross sections and R using CDF Run 2 Data", CDF note 6711.

[12] T. Nelson et al., "Forward Electron Tracking with the PhoenixMods Package", CDF note 6278.

[13] Al Goshaw, Helen Hayward, Beate Heinemann, Michael Kirby, Naho Tanimoto, "Inclusive W and Z selection in the Run II W/Z + gamma analysis", CDF note 6841.

[14] http://www-cdf.fnal.gov/internal/physics/photon/docs/cuts.html

[15] H. Hayward and B. Heinemann, "Determination of the QCD Jet Background to Isolated Photons ", CDF note 6363.

[16] H. Hayward and B. Heinemann, "Update of the Measurement of the Probability of a Jet faking an Isolated photon", CDF note 6838.

[17] Y.-K. Kim, J. Nielsen, L. Tompkins, G. Veramendi, "Trigger Efficiencies for High p_T Electrons", CDF note 6234.

[18] L. Cerrito, V. Martin, "Muon Cuts and Efficiencies for 4.11 Analyses", CDF note 6825.

[19] M. Coca and E. Halkiadakies, "Central Electron Identification Efficiencies for Winter 2003 conferences", CDF note 6850 and updated numbers from `http://www-cdf.fnal.gov/internal/physics/Winter03_nums.html`

[20] C. Issever et al., "Plug Electron Baseline Cuts and Efficiencies for Summer 2003", CDF note 6789.

[21] D. Goldstein et al., "A measurement of the ttbar cross-section using dileptons in the central and endplug detectors", CDF note 6588.

[22] S. Chuang et al., "Estimate of the amount of material in the CDF tracker using high-Pt electrons", CDF note 6573.

[23] M. Kirby, N. Tanimoto, et al. , "Underlying Event Studies and Photon ID Efficiencies in Run II", CDF note 6608.

[24] N. Tanimoto, D. Benjamin, A. Goshaw, M. Kirby, B. Heinemann, H. Hayward, "Efficiencies for $W\gamma$ analysis in Run 2", CDF note 6857.

[25] A. Hocker and W. Sakumoto, "Event $|Zvtx| < 60$ cm Cut Efficiency for Run II", CDF note 6331.

[26] J.-F. Arguin, B. Heinemann, A. Yagil, "The z-Vertex Algorithm in Run II", CDF note 6238.

[27] J.-F. Arguin, B. Heinemann, "Underlying Event Corrections in Run II", CDF note 6239.

[28] G. J. Feldman and R. D. Cousins, "A Unified Approach to the Classical Statistical Analysis of Smal Signals", Phys. Rev. D**57** (1998) 3873-3889.

[29] K. O. Mikaelia, M. A. Samuel and D. Sahdev, "Magnetic Moment of Weak Bosons Produced in pp and $p\bar{p}$ Collisions", Phys. Rev. Lett. **43**, 746 (1979).

[30] J. Ohnemus, "Order-α_s calculations of hadronic $W^{\pm}\gamma$ and $Z\gamma$ production", Phys. Rev. D **47**, 940 (1993); S. Mendoza, J. Smith, and W. L. van Neerven, Phys. Rev. D **47**, 3913 (1993).

[31] G.N. Valenzuela and J. Smith, "Experimental implications of finite-width and P_T effects in W -boson radiative production", Phys, Rev. D**31**, 2787 (1985).

[32] U. Baur, S. Errede, and G. Landsberg, "Rapidity correlations in $W\gamma$ production at hadron colliders", Phys. Rev. D**50**, 1917 (1994).